SUPPORTING INFORMATION

Evaluation of halogen bonding proclivity of oxazole derivatives carrying multiple acceptor sites in cocrystals with perfluorinated iodobenzenes

Ruđer Sušanj, Nikola Bedeković, Sara Cerovski, Nea Baus Topić, Vinko Nemec* and Dominik Cinčić*

Department of Chemistry, Faculty of Science, University of Zagreb, Horvatovac 102a, HR-10000 Zagreb, Croatia

E-mail: vnemec@chem.pmf.hr, dominik@chem.pmf.hr
Fax: +385 1 4606 341
Tel: +385 1 4606 362, +385 1 4606 379

Table of Contents

EXPERIMENTAL DETAILS

SYNTHESES OF ACCEPTORS

Acceptors have been synthesized by general procedure described in main text.

Exact equimolar amounts of aldehydes used are as follows:

Acceptor	Aldehyde	Volume used / µL
tfox	3-thiophenecarboxaldehyde	934
fox	3-furancarboxaldehyde	866
pox	3-pyridinecarboxaldehyde	940
tolox	4-methylbenzaldehyde	1180
nox	4-nitrobenzaldehyde	977
phox	benzaldehyde	1020

COCRYSTALLIZATION

Cocrystal of (**tfox**)$_2$(**14tfib**)

14tfib (40.1 mg, 0.100 mmol) was dissolved in a solvent mixture of 2.0 mL diethyl-ether and 2.0 mL of hexane followed by addition of 100 µL aliquot of **tfox** (sln, $c \approx 1$ mol dm^{-3}). The solution was left to crystallize at room temperature.

Cocrystal of (**tfox**)(**135tfib**)

135tfib (50.1 mg, 0.100 mmol) was dissolved in a 2.0 mL of ethyl-acetate, followed by addition of 100 µL aliquot of **tfox** (sln, $c \approx 1$ mol dm^{-3}). The solution was left to crystallize at room temperature.

Cocrystal of (**fox**)(**14tfib**)

14tfib (20.1 mg, 0.050 mmol) was dissolved in a solution mixture of 2.0 mL methyl-*tert*-butyl ether and 1.00 mL of methanol, followed by addition of 50 µL aliquot of **fox** (sln, $c \approx 1$ mol dm^{-3}). The solution was left to crystallize in partially closed vial at room temperature.

Cocrystal of (**fox**)(**135tfib**)

135tfib (51.0 mg, 0.100 mmol) was dissolved in a 2.0 mL of dichloromethane followed by addition of 100 µL aliquot of **fox** (sln, $c \approx 1$ mol dm^{-3}). The solution was left to crystallize at room temperature.

Cocrystal of (**pox**)(**14tfib**)

14tfib (40.1 mg, 0.100 mmol) was dissolved in 2.0 mL of chloroform, followed by addition of 100 µL aliquot of **pox** (sln, $c \approx 1$ mol dm^{-3}). The solution was left to crystallize at room temperature.

Cocrystal of (**pox**)(**135tfib**)

135tfib (51.0 mg, 0.100 mmol) was dissolved in in 2.0 mL of chloroform, followed by addition of 100 µL aliquot of **pox** (sln, $c \approx 1$ mol dm^{-3}). The solution was left to crystallize at room temperature.

Cocrystal of (**pox**)(**12tfib**)$_2$

12tfib (40.1 mg, 0.100 mmol) was dissolved in a solvent mixture of 1.0 mL methanol and 1.0 mL acetonitrile, followed by addition of 100 µL aliquot of **pox** (sln, $c \approx 1$ mol dm^{-3}). The solution was left to crystallize at room temperature.

Cocrystal of (**pox**)(**13tfib**)

13tfib (15 µL, 0.100 mmol) was dissolved in 2.00 mL of methyl-tert-butyl ether, followed by addition of 100 µL aliquot of **pox** (sln, $c \approx 1$ mol dm^{-3}). The solution was left to crystallize at room temperature.

Cocrystal of (**tolox**)(**14tfib**)

14tfib (40.1 mg, 0.100 mmol) was dissolved in a solvent mixture of 1.0 mL methanol and 1.0 mL acetonitrile followed by addition of 300 µL aliquot of **tolox** (sln, $c \approx 0.5$ mol dm^{-3}). The solution was left to crystallize at room temperature.

Cocrystal of (**tolox**)(**135tfib**)

135tfib (25.5 mg, 0.050 mmol) was dissolved in a solvent mixture of 1.0 mL methanol and 1.0 mL acetonitrile followed by addition of 300 µL aliquot of **tolox** (sln, $c \approx 0.5$ mol dm^{-3}). The solution was left to crystallize at room temperature.

Cocrystal of (**phox**)(**14tfib**)

14tfib (40.1 mg, 0.100 mmol) was dissolved in a solvent mixture of 1.0 mL ethanol and 1.0 mL methyl *tert*-butyl ether followed by addition of 100 µL aliquot of **phox** (sln, $c \approx 1.0$ mol dm^{-3}). The solution was left to crystallize at room temperature.

Cocrystal of (**phox**)(**135tfib**)

135tfib (51.0 mg, 0.100 mmol) was dissolved in a solvent mixture of 1.0 mL chloroform and 1.00 mL hexane followed by addition of 100 µL aliquot of **phox** (sln, $c \approx 1.0$ mol dm^{-3}). The solution was left to crystallize at room temperature.

Cocrystal of (**phox**)(**12tfib**)$_2$

12tfib (40.1 mg, 0.100 mmol) was dissolved in a solvent mixture of 2.00 mL methanol followed by addition of 100 µL aliquot of **phox** (sln, $c \approx 1$ mol dm^{-3}). The solution was left to crystallize at 4 °C.

Cocrystal of (**phox**)(**13tfib**)

13tfib (15 µL, 0.100 mmol) was dissolved in 1 mL diethyl ether and 1 mL of hexane, followed by addition of 100 µL aliquot of **phox** (sln, $c \approx 1$ mol dm^{-3}). The solution was left to crystallize at 4 °C.

Cocrystal of (**nox**)(**14tfib**)

A mixture containing **nox** (19.0 mg, 0.100 mol) and **14tfib** (40.1 mg, 0.100 mol) was dissolved in 4.00 mL of ethanol. The solution was left to crystallize at room temperature.

Cocrystal of (**nox**)(**135tfib**)

A mixture containing **nox** (19.0 mg, 0.100 mol) and **14tfib** (40.1 mg, 0.100 mol) was dissolved in a solvent mixture of 2.0 mL chloroform and 2.0 mL of hexane. The solution was left to crystallize at room temperature.

Cocrystal of (**box**)(**14tfib**)

14tfib (40.1 mg, 0.100 mmol) was dissolved in 2.0 mL of methanol followed by addition of 100 µL of melted **box**. The solution was left to crystallize at 4 °C.

Cocrystal of (**box**)$_3$(**135tfib**)

135tfib (51.0 mg, 0.100 mmol) was dissolved in 2.0 mL methanol followed by addition of 100 μL of melted **box**. The solution was left to crystallize at 4 °C.

Cocrystal of (**box**)(**12tfib**)

12tfib (40.1 mg, 0.100 mmol) was dissolved in 2.0 mL of methanol followed by addition of 100 μL of melted **box**. The solution was left to crystallize at 4 °C.

THERMAL ANALYSIS

DSC measurements were performed on a Mettler-Toledo DSC823e instrument. The samples were placed in sealed aluminium pans (40 μL) with a pinhole made in the top cover, and heated in flowing nitrogen (150 mL min^{-1}) from –10 °C to 300 °C for (**fox**)(**14tfib**), (**fox**)(**135tfib**), (**box**)(**14tfib**), (**box**)$_3$(**135tfib**), (**phox**)(**12tfib**)$_2$ and (**phox**)(**13tfib**); from 25 °C to -15 °C and then to 100 °C at two steps for **box** and from 25 °C to 300 °C for the rest of the samples, all at a rate of 10 °C min^{-1}. Data collection and analysis were performed using the program package STAR^e Software 17.00.[1]

POWDER X-RAY DIFFRACTION EXPERIMENTS

PXRD experiments were performed on a Malvern PANalytical *Aeris* X-ray diffractometer with Cu$K_{\alpha1}$ (1.54056 Å) radiation at 15 mA and 40 kV. The scattered intensities were measured with a line (1D) detector. The angular range was from 5 to 40° (2θ) with an interpolated step size of 0.00543322°. Data analysis was performed using the program *Data Viewer*.[3]

SINGLE-CRYSTAL X-RAY DIFFRACTION EXPERIMENTS

The crystal and molecular structures of the prepared cocrystals were determined by single crystal X-ray diffraction. Details of data collection and crystal structure refinement are listed in Table S1, S2, S3 and S4. Diffraction measurements were made on and Rigaku Synergy XtaLAB X-ray diffractometer with graphite-monochromated MoK_α (λ = 0.71073Å) radiation. The data sets were collected using the ω scan mode over the 2θ range up to 64°. The CrysAlisPro program package was employed for data collection, cell refinement, and data reduction.[4] The structures were solved by direct methods and refined using the SHELXS, SHELXT, and SHELXL programs, respectively.[5,6] The structural refinement was performed on F^2

using all data. Hydrogen atoms were placed in calculated positions and treated as riding on their parent atoms All calculations were performed using the WINGX[7] or Olex2[8] crystallographic suite of programs. The molecular structures of compounds and their molecular packing projections were prepared by Mercury.[9]

References

1. STARe Evaluation Software Version 17.00. Mettler–Toledo GmbH, 2022.
2. Data Viewer Version 1.9a, PANalytical B.V. Almelo, The Netherlands, 2018.
3. Omnic Specta Software 9.9.549, Thermo Fisher Scientific, 2018.
4. Rigaku Oxford Diffraction, Gemini CCD system, CrysAlis Pro software, Version 171.41.93a, 2020.
5. (a) G. M. Sheldrick, *Acta Cryst. A*, 2008, **64**, 112–122; (b) G. M. Sheldrick, *Acta Cryst. C*, 2015, **71**, 3–8.
6. G. M. Sheldrick, *Acta Cryst. A*, 2015, **71**, 3–8.
7. L. J. Farrugia, *J. Appl. Cryst.*, 2012, **45**, 849–854.
8. O. V. Dolomanov, L. J. Bourhis, R. J. Gildea, J. A. K. Howard, H. Puschmann, *J. Appl. Cryst.*, 2009, **42**, 339–341.
9. C. F. Macrae, I. J. Bruno, J. A. Chisholm, P. R. Edgington, P. McCabe, E. Pidcock, L. Rodriguez-Monge, R. Taylor, J. v. d. Streek and P. A. Wood, *J. Appl. Crystallogr.* **2008**, 41, 466.

Table S1. Crystal data and refinement details for the prepared compounds.

	(tfox)$_2$(14tfib)	**(tfox)(135tfib)**
Molecular formula	$(C_7H_5NOS)_2(C_6F_4I_2)$	$(C_7H_5NOS)(C_6F_3I_3)$
M_r	704.22	660.94
Crystal system	triclinic	triclinic
Space group	$P\,\bar{1}$	$P\,\bar{1}$
Crystal data:		
a / Å	5.8434(3)	9.1407(2)
b / Å	9.8958(4)	9.6712(3)
c / Å	10.8439(5)	10.5728(2)
α / °	68.788(4)	83.925(2)
β / °	84.873(4)	86.217(2)
γ / °	75.319(4)	65.675(3)
V / Å^3	565.48(5)	846.64(4)
Z	1	2
D_{calc} / g cm^{-3}	2.068	2.593
λ(MoK_α) / Å	0.71073	0.71073
T / K	294.98(10)	295.00(10)
Crystal size / mm^3	0.44x0.20x0.13	0.50x0.31x0.09
μ / mm^{-1}	3.019	5.689
F(000)	334	600
Refl. collected/unique	12008/3927	20245/5899
Parameters/restraints	145/0	237/28
$\Delta\rho_{max}$, $\Delta\rho_{min}$ / e Å^{-3}	0.841, –0.466	0.777, –1.319
$R[F^2 > 4\sigma(F^2)]$	0.0305	0.0341
w$R(F^2)$	0.0843	0.0907
Goodness-of-fit, S	1.044	1.071

Table S1. Continued

	(fox)(14tfib)	**(fox)(135tfib)**
Molecular formula	$(C_7H_5NO_2)(C_6F_4I_2)$	$(C_7H_5NO_2)(C_6F_3I_3)$
M_r	536.98	644.88
Crystal system	monoclinic	monoclinic
Space group	$P\,2_1$	$C\,c$
Crystal data:		
a / Å	5.7685(5)	4.9817(2)
b / Å	16.8433(9)	17.5239(4)
c / Å	7.91999(5)	19.04049(7)
α / °	90	90
β / °	97.137(7)	93.994(3)
γ / °	90	90
V / Å^3	763.54(9)	1658.21(10)
Z	2	4
D_{calc} / g cm^{-3}	2.336	2.583
λ(MoK_α) / Å	0.71073	0.71073
T / K	295	294.99(10)
Crystal size / mm^3	0.54x0.28x0.07	0.54x0.32x0.16
μ / mm^{-1}	4.166	5.688
F(000)	496	1168
Refl. Collected/unique	3182/2022	21219/5487
Parameters/restraints	199/1	200/2
$\Delta\rho_{max}$, $\Delta\rho_{min}$ / e Å^{-3}	0.481, –0.444	1.108,–1.477
$R[F^2 > 4\sigma(F^2)]$	0.0428	0.0333
w$R(F^2)$	0.0777	0.0909
Goodness-of-fit, S	1.009	1.084

Table S1. Continued

	(pox)(14tfib)	**(pox)(135tfib)**	**(pox)(12tfib)$_2$**	**(pox)(13tfib)**
Molecular formula	$(C_8H_6N_2O)(C_6F_4I_2)$	$(C_8H_6N_2O)(C_6F_3I_3)$	$(C_8H_6N_2O)(C_6F_4I_2)_2$	$(C_8H_6N_2O)(C_6F_4I_2)$
M_r	548.01	655.91	949.87	548.01
Crystal system	orthorhombic	monoclinic	monoclinic	orthorhombic
Space group	*P bcn*	*P* $2_1/n$	*P* $2_1/n$	*P* $2_12_12_1$
Crystal data:				
a / Å	17.9765(13)	4.9988(3)	7.3099(5)	5.99780(10)
b / Å	12.8650(13)	17.7100(8)	12.9537(11)	7.7740(2)
c / Å	13.6805(10)	19.4968(10)	26.1341(15)	32.9740(7)
α / °	90	90	90	90
β / °	90	95.150(5)	90.842(6)	90
γ / °	90	90	90	90
V / Å^3	3163.9(5)	1719.06(16)	2474.4(3)	1537.48(6)
Z	8	4	4	4
D_{calc} / g cm^{-3}	2.301	2.534	2.550	2.367
λ(MoK_α) / Å	0.71073	0.71073	0.71073	0.71073
T / K	295	295	295	169.99(10)
Crystal size / mm^3	0.83x0.31x0.18	0.98x0.53x0.23	0.81x0.47x0.18	0.333x0.138x0.046
μ / mm^{-1}	4.021	5.487	5.114	4.137
F(000)	2032	1192	1728	1016
Refl. Collected/unique	26107/2773	16079/3748	18802/4346	28925/4483
Parameters/restraints	208/0	208/0	316/0	209/0
$\Delta\rho_{max}$, $\Delta\rho_{min}$ / e Å^{-3}	1.692, –1.232	1.354, –1.798	2.421, –0.796	0.316, –0.365
$R[F^2 > 4\sigma(F^2)]$	0.0657	0.0556	0.0748	0.0187
w$R(F^2)$	0.2040	0.1214	0.1927	0.0364
Goodness-of-fit, *S*	1.074	1.181	1.065	1.030

Table S1. Continued

	(tolox)(14tfib)	**(tolox)(135tfib)**
Molecular formula	$(C_{10}H_9NO)(C_6F_4I_2)$	$(C_{10}H9NO)(C_6F_3I_3)$
M_r	561.04	668.94
Crystal system	monoclinic	monoclinic
Space group	*P* 2_1	*C c*
Crystal data:		
a / Å	9.0215(11)	17.6258(2)
b / Å	5.9752(6)	4.72480(10)
c / Å	16.633(2)	22.8559(3)
α / °	90	90
β / °	102.764(12)	97.2400(10)
γ / °	90	90
V / Å^3	874.46(18)	1888.23(5)
Z	2	4
D_{calc} / g cm^{-3}	2.131	2.353
λ(MoK_α) / Å	0.71073	0.71073
T / K	295	295
Crystal size / mm^3	0.89x0.48x0.36	0.84x0.19x0.12
μ / mm^{-1}	3.638	4.996
F(000)	524	1224
Refl. collected/unique	9976/5634	137954/6510
Parameters/restraints	218/1	218/2
$\Delta\rho_{max}$, $\Delta\rho_{min}$ / e Å^{-3}	0.589, –0.417	1.067, –1.012
$R[F^2 > 4\sigma(F^2)]$	0.0368	0.0417
w$R(F^2)$	0.0815	0.1233
Goodness-of-fit, *S*	1.024	1.032

Table S1. continued

	nox
Molecular formula	$C_9H_6N_2O_3$
M_r	190.16
Crystal system	monoclinic
Space group	*C* 2/*c*
Crystal data:	
a / Å	19.0306(7)
b / Å	6.4052(2)
c / Å	14.0416(5)
α / °	90
β / °	102.248(4)
γ / °	90
V / Å^3	1672.64(10)
Z	8
D_{calc} / g cm^{-3}	1.510
λ(MoK_α) / Å	0.71073
T / K	295
Crystal size / mm^3	0.92x0.70x0.50
μ / mm^{-1}	0.117
F(000)	784
Refl. collected/unique	17343/2860
Parameters/restraints	127/0
$\Delta\rho_{max}$, $\Delta\rho_{min}$ / e Å^{-3}	0.218, –0.200
$R[F^2 > 4\sigma(F^2)]$	0.0504
w$R(F^2)$	0.1500
Goodness-of-fit, *S*	1.019

Table S1. continued

	(nox)(14tfib)	**(nox)(135tfib)**
Molecular formula	$(C_9H_6N_2O_3)(C_6F_4I_2)$	$(C_9H_6N_2O_3)(C_6F_3I_3)$
M_r	592.02	699.92
Crystal system	monoclinic	monoclinic
Space group	$P\,2_1/n$	$C\,c$
Crystal data:		
a / Å	8.7028(3)	4.9443(2)
b / Å	21.0309(10)	17.6264(6)
c / Å	9.4060(3)	21.8090(9)
α / °	90	90
β / °	95.139(4)	96.092(4)
γ / °	90	90
V / Å^3	1714.64(12)	1889.93(13)
Z	4	4
D_{calc} / g cm^{-3}	2.293	2.460
λ(MoK_α) / Å	0.71073	0.71073
T / K	295	298.14(10)
Crystal size / mm^3	0.66x0.23x0.08	0.59x0.19x0.10
μ / mm^{-1}	3.728	5.007
F(000)	1104	1280
Refl. collected/unique	14295/3717	8160/3592
Parameters/restraints	235/0	235/2
$\Delta\rho_{max}$, $\Delta\rho_{min}$ / e Å^{-3}	0.548 , –0.760	0.900, –0.869
$R[F^2 > 4\sigma(F^2)]$	0.0357	0.0302
w$R(F^2)$	0.0599	0.0748
Goodness-of-fit, S	1.017	1.073

Table S1. continued

	box
Molecular formula	C_7H_5NO
M_r	119.12
Crystal system	monoclinic
Space group	*C* 2/*c*
Crystal data:	
a / Å	11.7125(4)
b / Å	8.7742(3)
c / Å	22.0600(8)
α / °	90
β / °	98.273(3)
γ / °	90
V / Å^3	2243.47(14)
Z	16
D_{calc} / g cm^{-3}	1.411
λ(MoK_α) / Å	0.71073
T / K	169.99(0)
Crystal size / mm^3	0.636x0.564x0.123
μ / mm^{-1}	0.097
F(000)	992
Refl. collected/unique	12585/3284
Parameters/restraints	163/0
$\Delta\rho_{max}$, $\Delta\rho_{min}$ / e Å^{-3}	0.253, –0.316
$R[F^2 > 4\sigma(F^2)]$	0.0426
w$R(F^2)$	0.1231
Goodness-of-fit, *S*	1.082

Table S1. continued

	(box)(14tfib)	**(box)$_3$(135tfib)**	**(box)(12tfib)**
Molecular formula	$(C_7H_5NO)(C_6F_4I_2)$	$(C_7H_5NO)_3(C_6F_3I_3)$	$(C7H_5NO)(C_6F_4I_2)$
M_r	520.98	867.12	520.98
Crystal system	monoclinic	triclinic	monoclinic
Space group	$P\,2_1/n$	$P\,-1$	$P\,2_1/n$
Crystal data:			
a / Å	14.1322(4)	10.0238(5)	14.4917(3)
b / Å	5.5319(2)	11.0764(5)	7.3816(2)
c / Å	18.6410(5)	12.9002(4)	26.3414(5)
α / °	90	99.313(3)	90
β / °	95.506(3)	95.503(3)	90.223(2)
γ / °	90	94.395(4)	90
V / Å^3	1450.59(8)	1400.68(10)	2817.77(11)
Z	4	2	8
D_{calc} / g cm^{-3}	2.376	2.056	2.456
λ(MoK_α) / Å	0.71073	0.71073	0.71073
T / K	150(2)	169.99(10)	169.99(10)
Crystal size / mm^3	0.35x0.30x0.22	0.77x0.54x0.20	0.58x0.08x0.07
μ / mm^{-1}	4.373	3.401	4.506
F(000)	956	816	1920
Refl. collected/unique	15556/3155	31744/9710	46796/9684
Parameters/restraints	190/0	352/0	379/0
$\Delta\rho_{max}$, $\Delta\rho_{min}$ / e Å^{-3}	0.533, –0.764	3.007, –2.140	0.952, –0.865
$R[F^2 > 4\sigma(F^2)]$	0.0269	0.0607	0.0287
w$R(F^2)$	0.0698	0.1870	0.0635
Goodness-of-fit, S	0.932	1.033	1.027

	(phox)(14tfib)	**(phox)(135tfib)**	**(phox)(12tfib)$_2$**	**(phox)(13tfib)**
Molecular formula	$(C_9H_7NO)(C_6F_4I_2)$	$(C_9H_7NO)(C_6F_3I_3)$	$(C_9H_7NO)(C_6F_4I_2)_2$	$(C_9H_7NO)(C_6F_4I_2)$
M_r	547.02	654.92	948.88	547.02
Crystal system	monoclinic	triclinic	monoclinic	triclinic
Space group	$P\,2_1$	$P\,\bar{1}$	$C\,2/c$	$P\,\bar{1}$
Crystal data:				
a / Å	8.1546(5)	9.1993(4)	29.7446(14)	8.1512(3)
b / Å	5.9866(3)	9.7631(4)	8.7558(2)	9.2659(4)
c / Å	16.6160(7)	10.5954(3)	24.0108(11)	11.0875(4)
α / °	90	84.563(3)	90	103.811(3)
β / °	97.011(5)	85.979(3)	127.927(7)	95.582(3)
γ / °	90	65.091(4)	90	101.302(3)
V / Å^3	805.10(7)	858.73(6)	4932.6(5)	788.26(5)
Z	2	2	8	2
D_{calc} / g cm^{-3}	2.256	2.533	2.555	2.305
λ(MoK_α) / Å	0.71073	0.71073	0.71073	0.71073
T / K	295	298.09(10)	170.00(10)	169.99(10)
Crystal size / mm^3	0.58x0.33x0.06	0.73x0.52x0.31	0.39x0.327x0.074	0.412x0.232x0.139
μ / mm^{-1}	3.949	5.490	5.130	4.033
F(000)	508	596	3456	508
Refl. collected/unique	17587/5574	19979/5968	48908/7186	14109/4595
Parameters/restraints	208/1	208/0	316/0	208/0
$\Delta\rho_{max}$, $\Delta\rho_{min}$ / e Å^{-3}	0.708, –0.365	1.248, –1.416	1.720, –1.612	0.762, –0.609
$R[F^2 > 4\sigma(F^2)]$	0.0356	0.0405	0.0249	0.0276
w$R(F^2)$	0.1009	0.1126	0.0519	0.0565
Goodness-of-fit, S	0.990	1.040	1.010	1.043

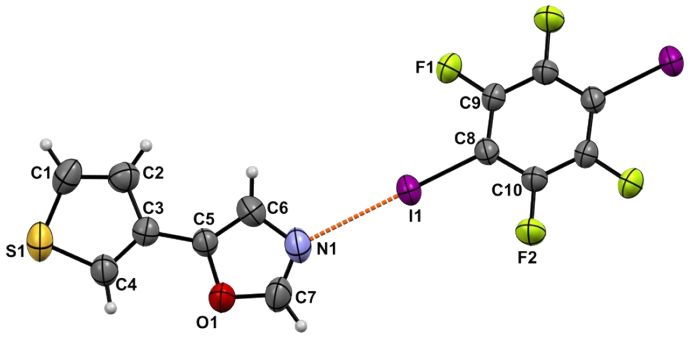

Figure S1. Partial molecular structure of (**tfox**)$_2$(**14tfib**) showing the atom-labelling scheme. Displacement ellipsoids are drawn at the 50 % probability level, and H atoms are shown as small spheres of arbitrary radius.

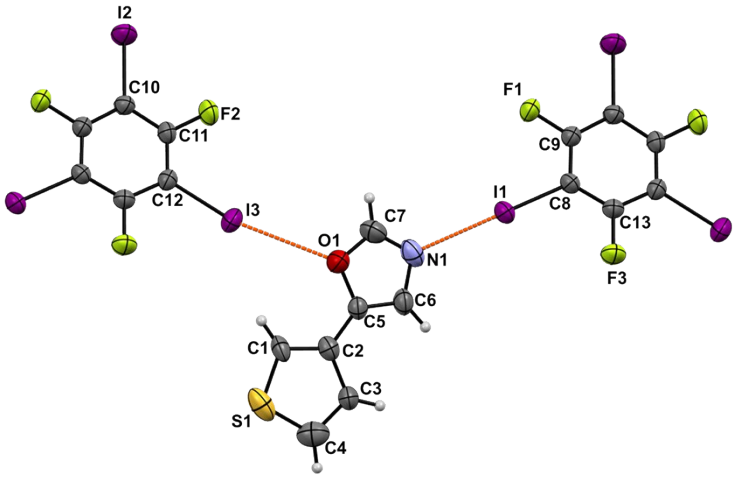

Figure S2. Partial molecular structure of (**tfox**)(**135tfib**) showing the atom-labelling scheme. Displacement ellipsoids are drawn at the 50 % probability level, and H atoms are shown as small spheres of arbitrary radius.

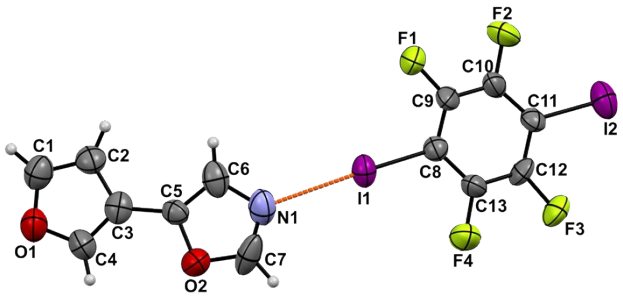

Figure S3. Partial molecular structure of (**fox**)(**14tfib**) showing the atom-labelling scheme. Displacement ellipsoids are drawn at the 50 % probability level, and H atoms are shown as small spheres of arbitrary radius.

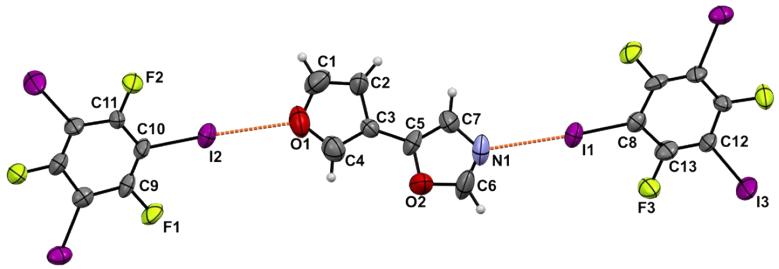

Figure S4. Partial molecular structure of (**fox**)(**135tfib**) showing the atom-labelling scheme. Displacement ellipsoids are drawn at the 50 % probability level, and H atoms are shown as small spheres of arbitrary radius.

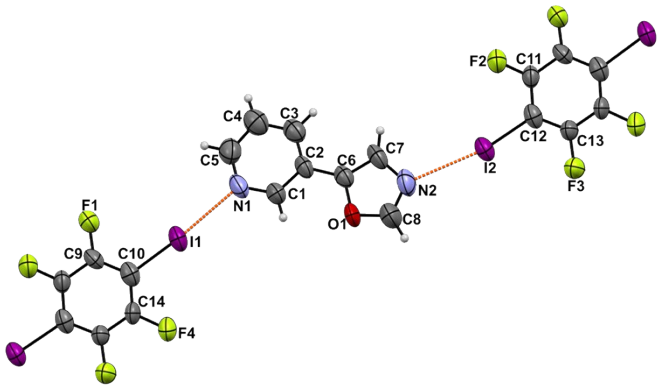

Figure S5. Partial molecular structure of (**pox**)(**14tfib**) showing the atom-labelling scheme. Displacement ellipsoids are drawn at the 50 % probability level, and H atoms are shown as small spheres of arbitrary radius.

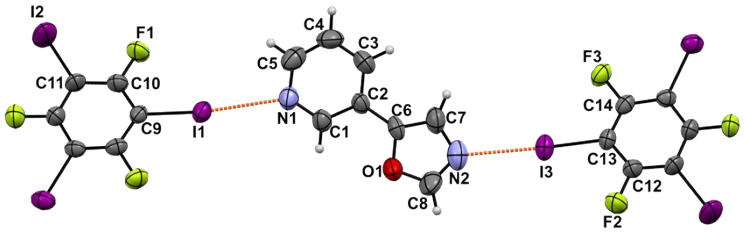

Figure S6. Partial molecular structure of (**pox**)(**135tfib**) showing the atom-labelling scheme. Displacement ellipsoids are drawn at the 50 % probability level, and H atoms are shown as small spheres of arbitrary radius.

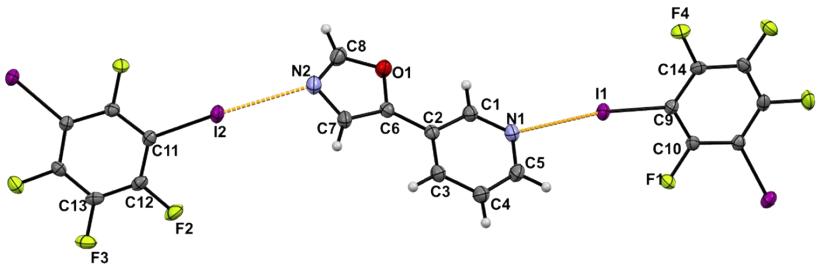

Figure S7. Partial molecular structure of (**pox**)(**13tfib**) showing the atom-labelling scheme. Displacement ellipsoids are drawn at the 50 % probability level, and H atoms are shown as small spheres of arbitrary radius.

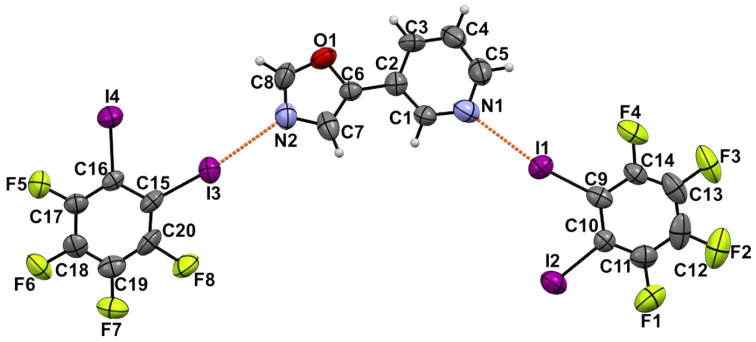

Figure S8. Partial molecular structure of (**pox**)(**12tfib**)$_2$ showing the atom-labelling scheme. Displacement ellipsoids are drawn at the 50 % probability level, and H atoms are shown as small spheres of arbitrary radius.

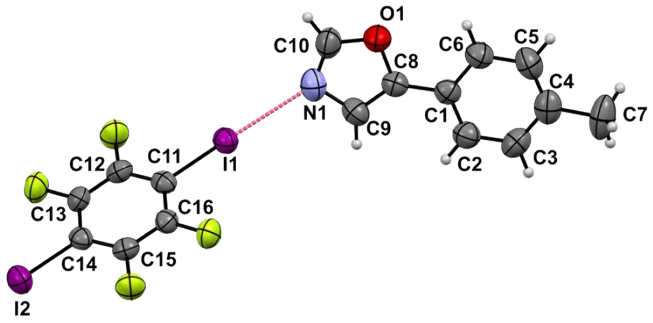

Figure S9. Partial molecular structure of (**tolox**)(**14tfib**) showing the atom-labelling scheme. Displacement ellipsoids are drawn at the 50 % probability level, and H atoms are shown as small spheres of arbitrary radius.

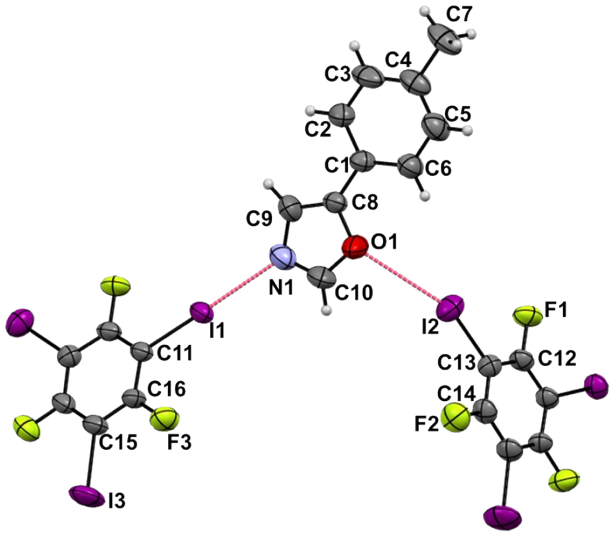

Figure S10. Partial molecular structure of (**tolox**)(**135tfib**) showing the atom-labelling scheme. Displacement ellipsoids are drawn at the 50 % probability level, and H atoms are shown as small spheres of arbitrary radius.

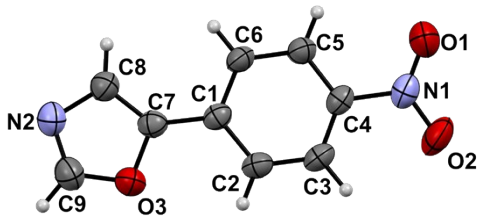

Figure S11. Molecular structure of **nox** showing the atom-labelling scheme. Displacement ellipsoids are drawn at the 50 % probability level, and H atoms are shown as small spheres of arbitrary radius.

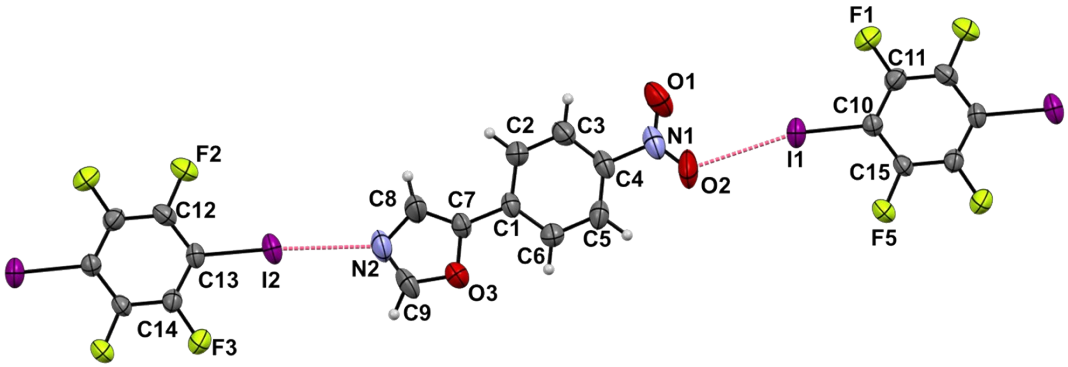

Figure S12. Molecular structure of (**nox**)(**14tfib**) showing the atom-labelling scheme. Displacement ellipsoids are drawn at the 50 % probability level, and H atoms are shown as small spheres of arbitrary radius.

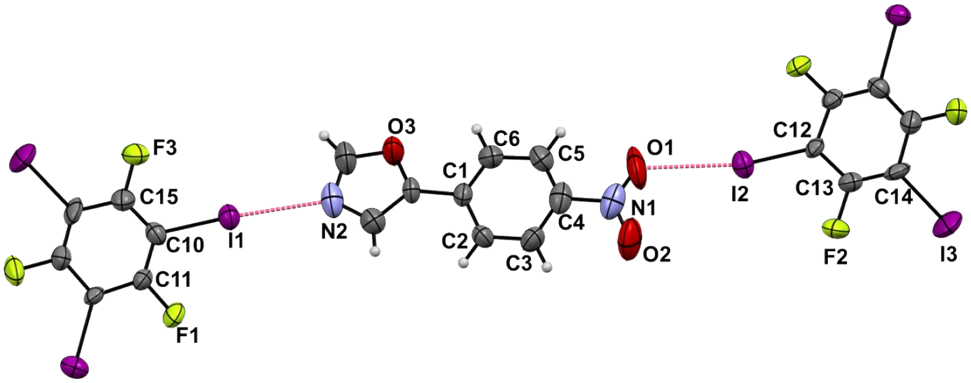

Figure S13. Molecular structure of (**nox**)(**135tfib**) showing the atom-labelling scheme. Displacement ellipsoids are drawn at the 50 % probability level, and H atoms are shown as small spheres of arbitrary radius.

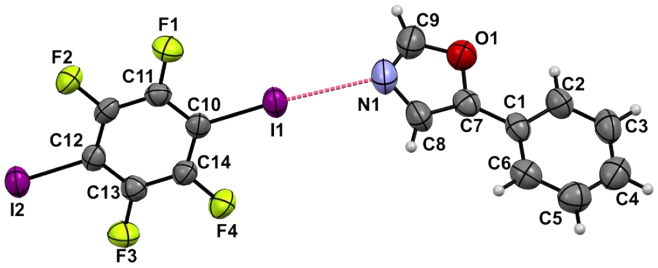

Figure S14. Molecular structure of (**phox**)(**14tfib**) showing the atom-labelling scheme. Displacement ellipsoids are drawn at the 50 % probability level, and H atoms are shown as small spheres of arbitrary radius.

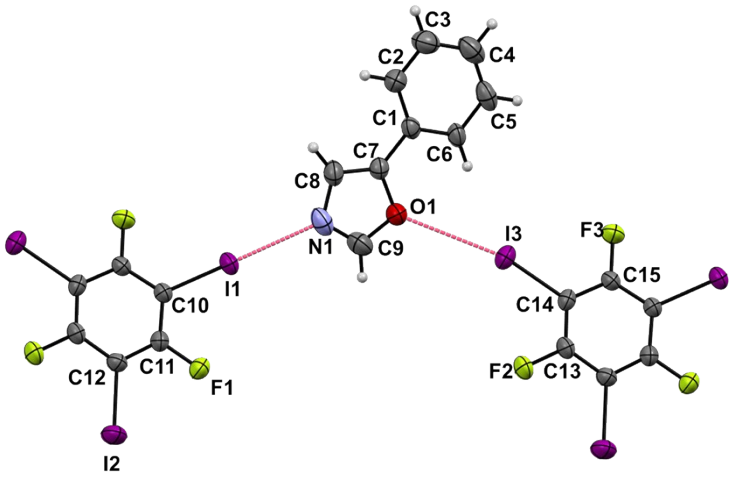

Figure S15. Molecular structure of (**phox**)(**135tfib**) showing the atom-labelling scheme. Displacement ellipsoids are drawn at the 50 % probability level, and H atoms are shown as small spheres of arbitrary radius.

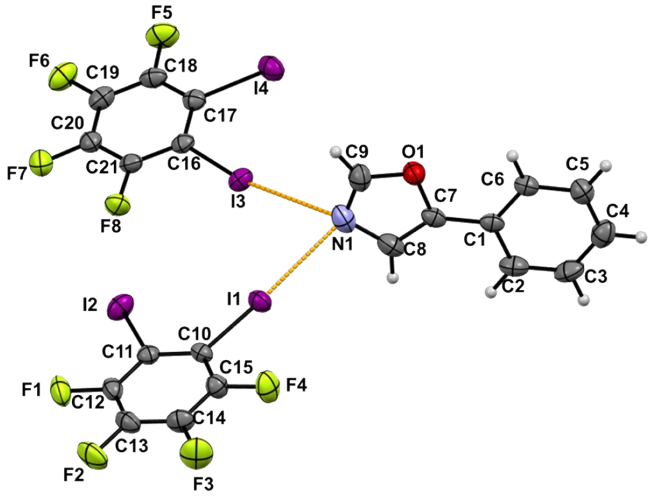

Figure S16. Molecular structure of (**phox**)(**12tfib**)$_2$ showing the atom-labelling scheme. Displacement ellipsoids are drawn at the 50 % probability level, and H atoms are shown as small spheres of arbitrary radius.

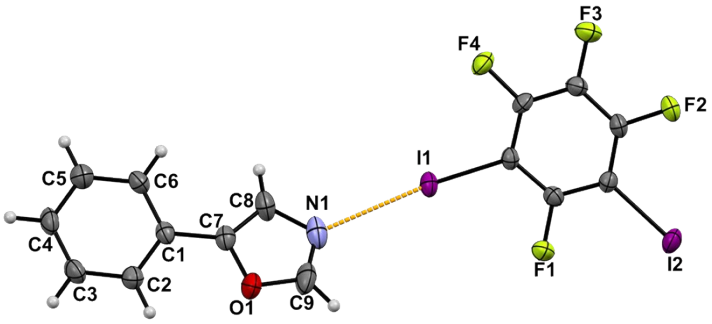

Figure S17. Molecular structure of (**phox**)(**13tfib**) showing the atom-labelling scheme. Displacement ellipsoids are drawn at the 50 % probability level, and H atoms are shown as small spheres of arbitrary radius.

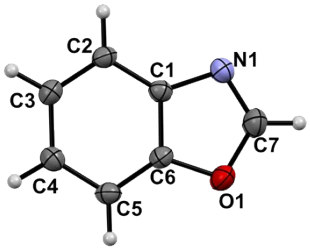

Figure S18. Molecular structure of **box** showing the atom-labelling scheme. Displacement ellipsoids are drawn at the 50 % probability level, and H atoms are shown as small spheres of arbitrary radius.

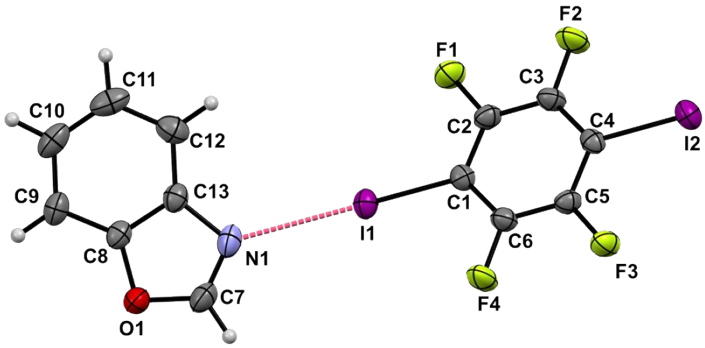

Figure S19. Molecular structure of (**box**)(**14tfib**) showing the atom-labelling scheme. Displacement ellipsoids are drawn at the 50 % probability level, and H atoms are shown as small spheres of arbitrary radius.

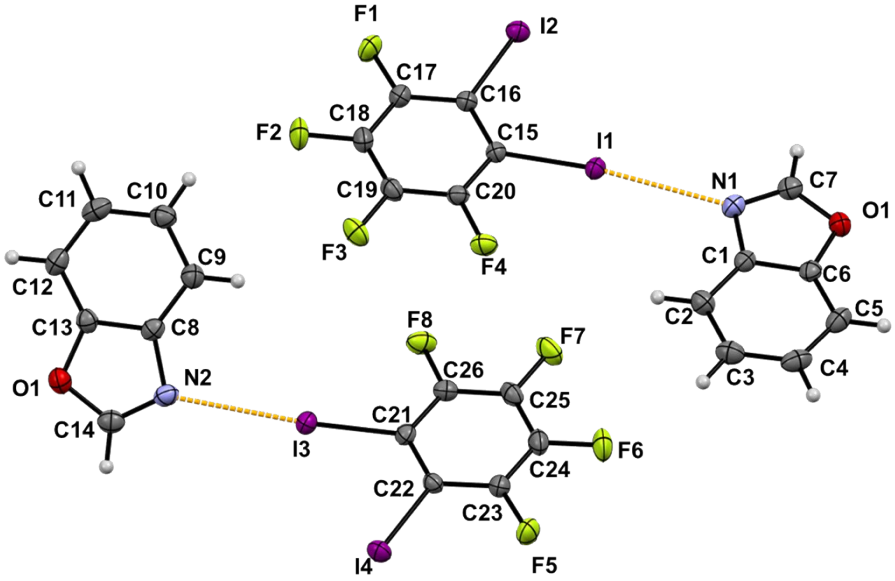

Figure S20. Molecular structure of (**box**)(**12tfib**) showing the atom-labelling scheme. Displacement ellipsoids are drawn at the 50 % probability level, and H atoms are shown as small spheres of arbitrary radius.

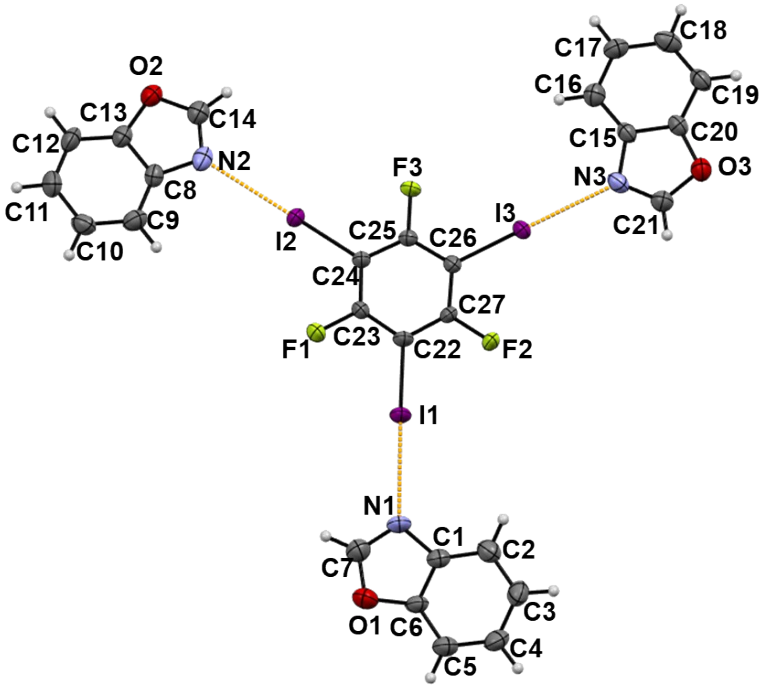

Figure S21. Molecular structure of (**box**)$_3$(**135tfib**) showing the atom-labelling scheme. Displacement ellipsoids are drawn at the 50 % probability level, and H atoms are shown as small spheres of arbitrary radius.

Table S2. Melting / decomposition temperatures of prepared cocrystals or crystal phases obtained by cocrystallized reactants in determined stoichiometry.

Compound	Onset melting / decomposition temperature
(**tfox**)$_2$(**14tfib**)	54.7 °C
(**tfox**)(**135tfib**)	81.2 °C
fox + **14tfib**	98.9 °C
fox + **135tfib**	145.9 °C
pox + **14tfib**	93.8 °C
pox + **135tfib**	122.6 °C
pox + **12tfib**(2 eq)	36.5 °C and 51.3 °C
pox+**13tfib**	94.3 °C
tolox + **14tfib**	73.8 °C
(**phox**)(**14tfib**)	81.6 °C
phox + **12tfib**(2 eq)	28.9 °C
phox+ **13tfib**	45.3 °C
(**phox**)(**135tfib**)	107.5 °C
nox + **14tfib**	105.4 °C
nox +**135tfib**	162.3 °C
box + **14tfib**	24.3 °C
box + **12tfib**	57.6 °C
box (3eq.) + **135tfib**	44.9 °C

DSC Curves with Indicated Onset Temperatures

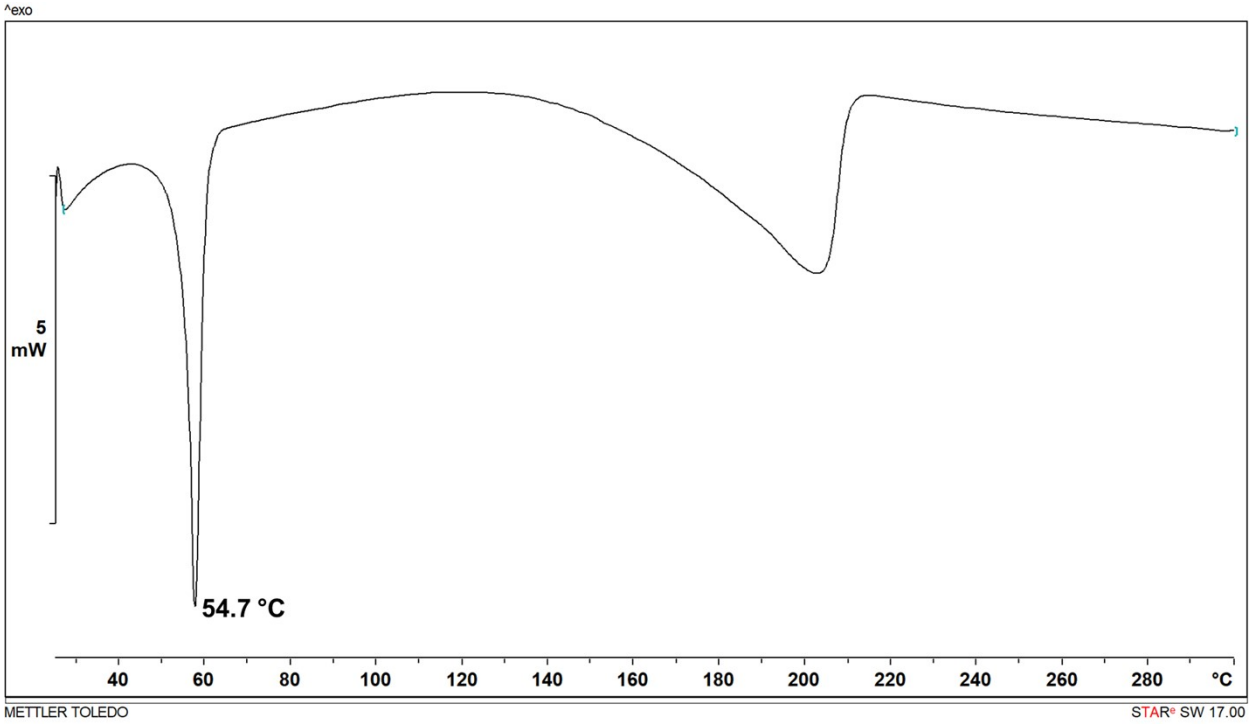

Figure S22. DSC curve of (**tfox**)$_2$(**14tfib**)

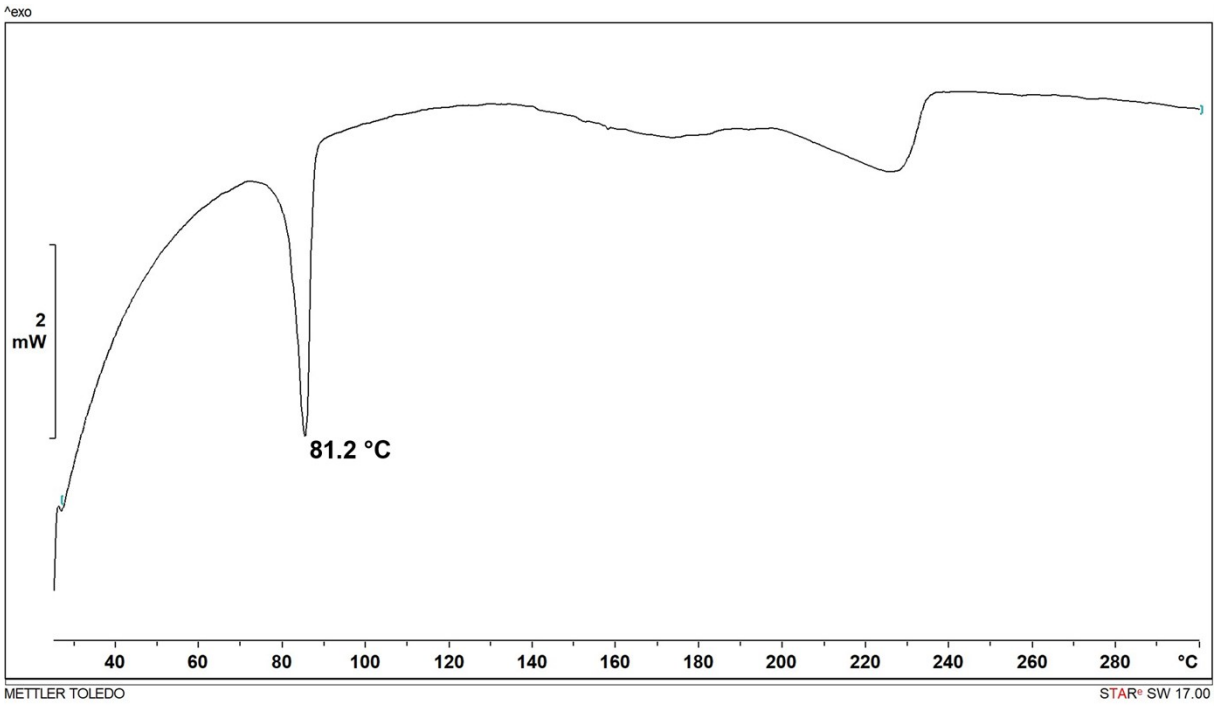

Figure S23. DSC curve of (**tfox**)(**135tfib**)

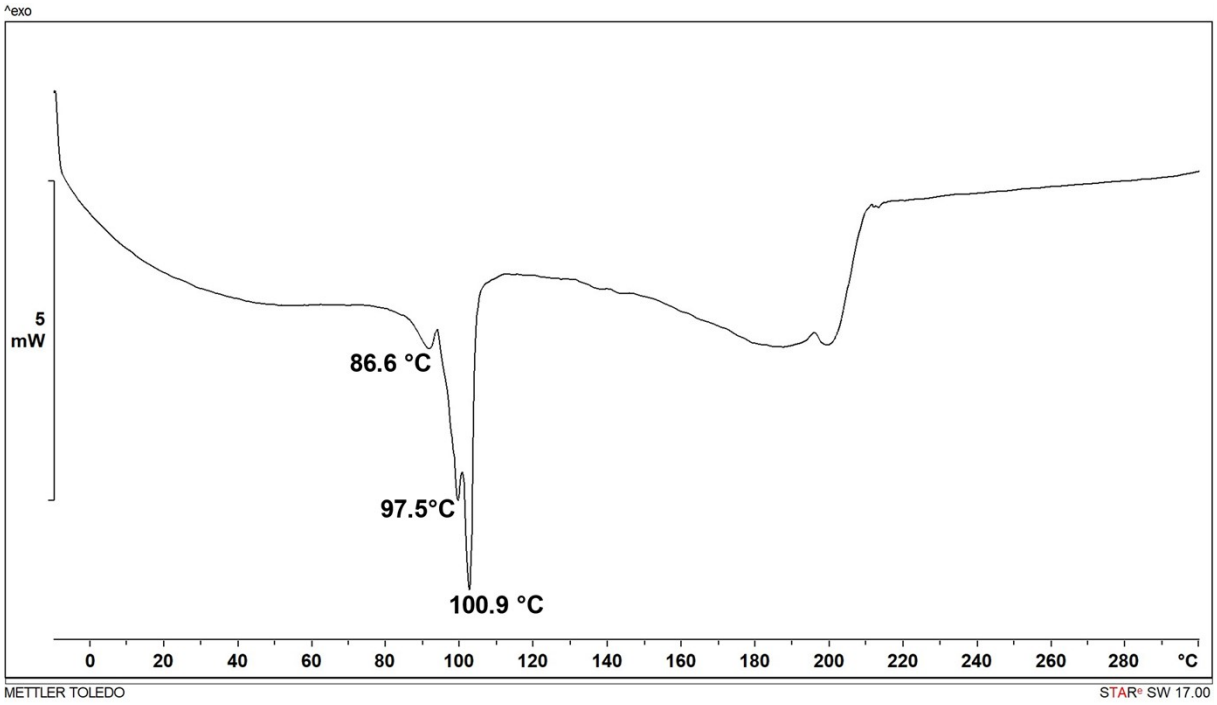

Figure S24. DSC curve of or crystal phase obtained by cocrystallized **fox** and **14tfib** in their respective stoichiometry.

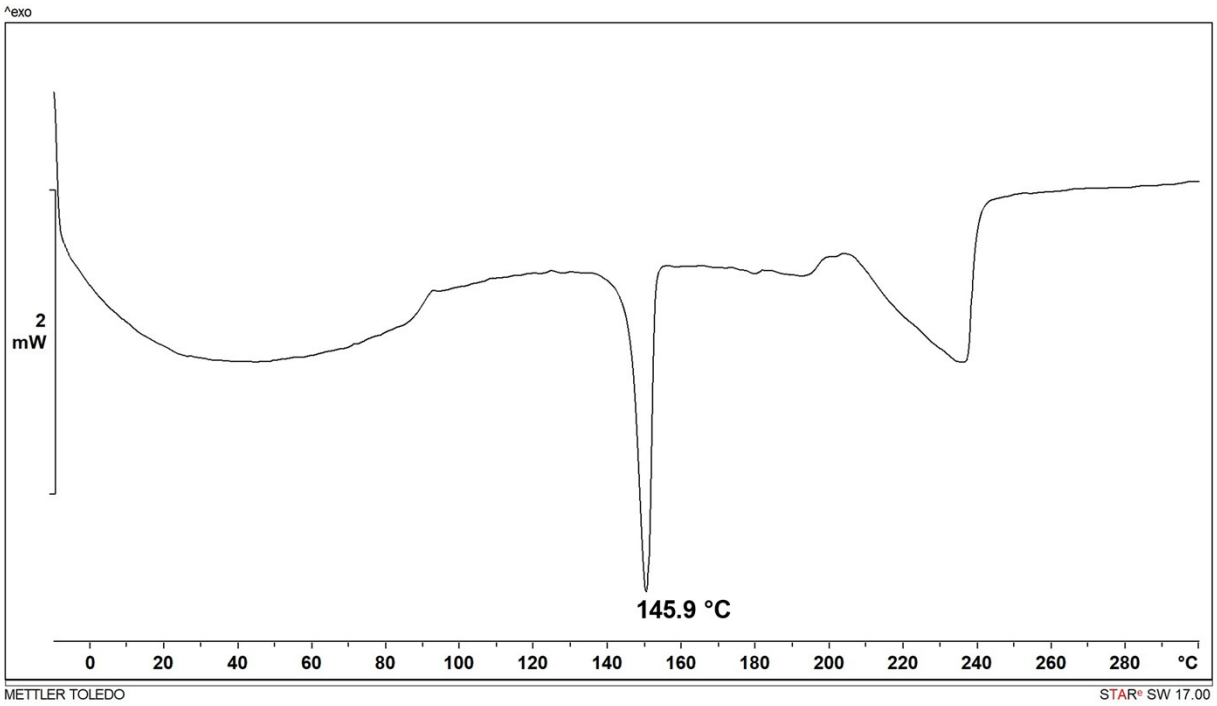

Figure S25. DSC curve of or crystal phase obtained by cocrystallized **fox** and **135tfib** in their respective stoichiometry

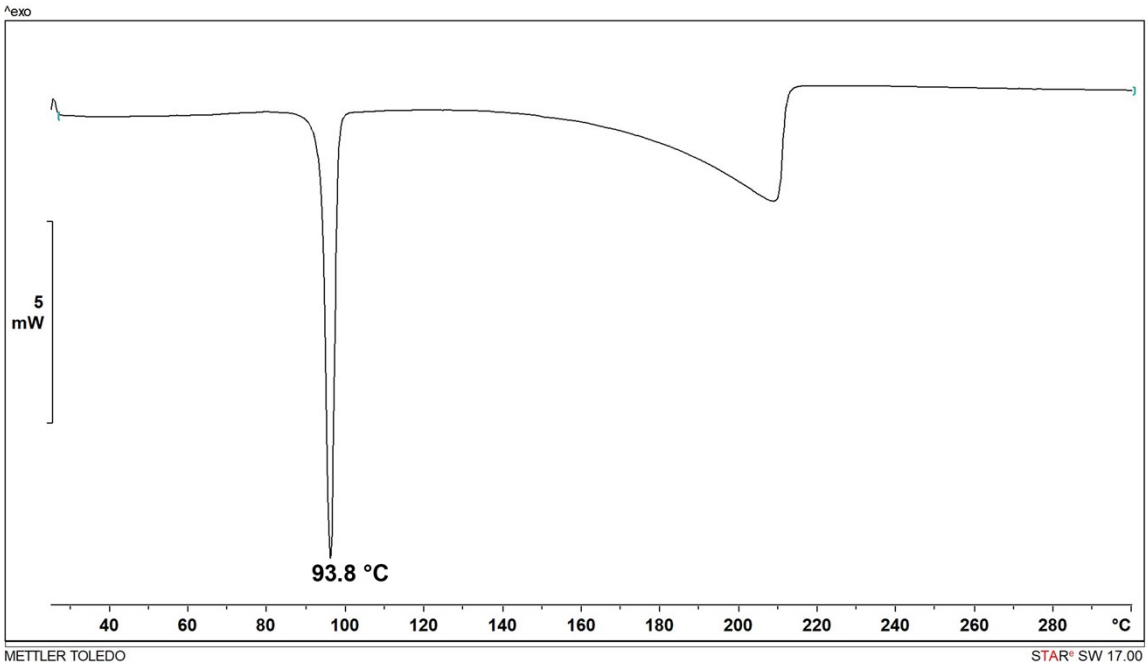

Figure S26. DSC curve of or crystal phases obtained by cocrystallized **pox** and **14tfib** in their respective stoichiometry.

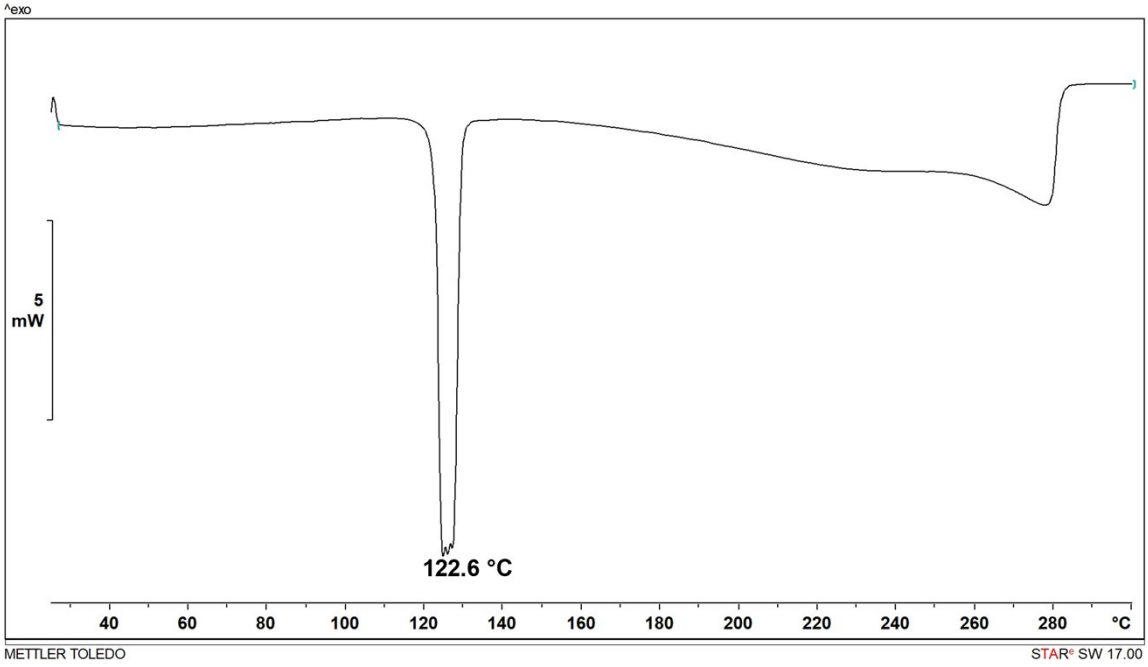

Figure S27. DSC curve of or crystal phases obtained by cocrystallized **fox** and **135tfib** in their respective stoichiometry

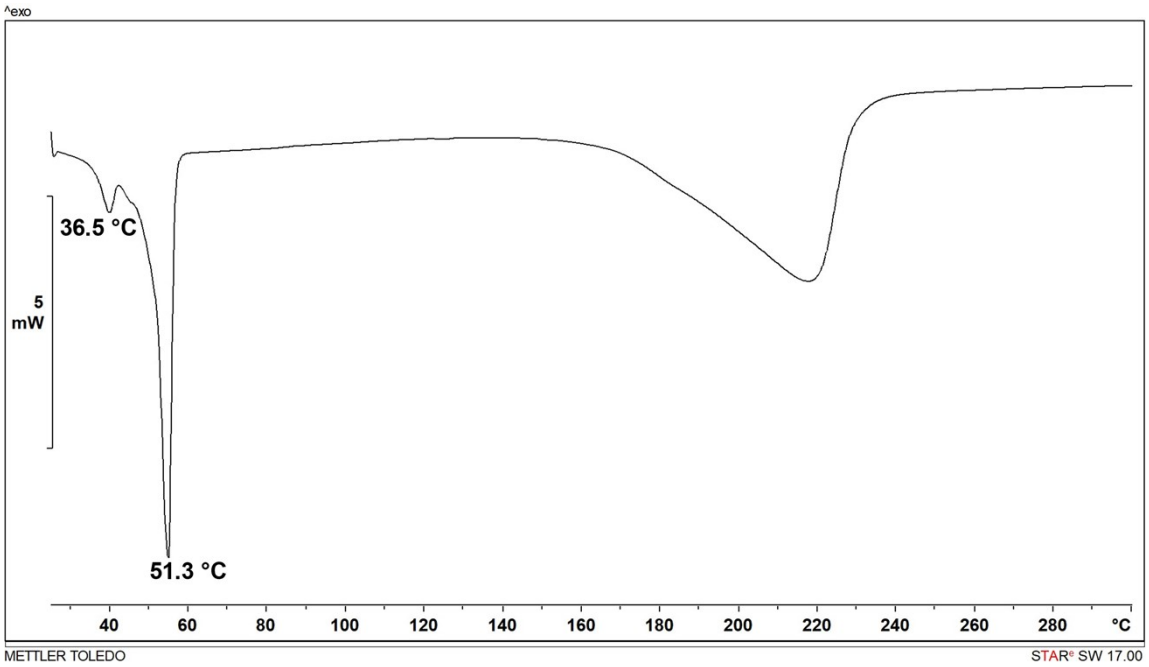

Figure S28. DSC curve of or crystal phases obtained by cocrystallized **pox** and **12tfib** in their respective stoichiometry.

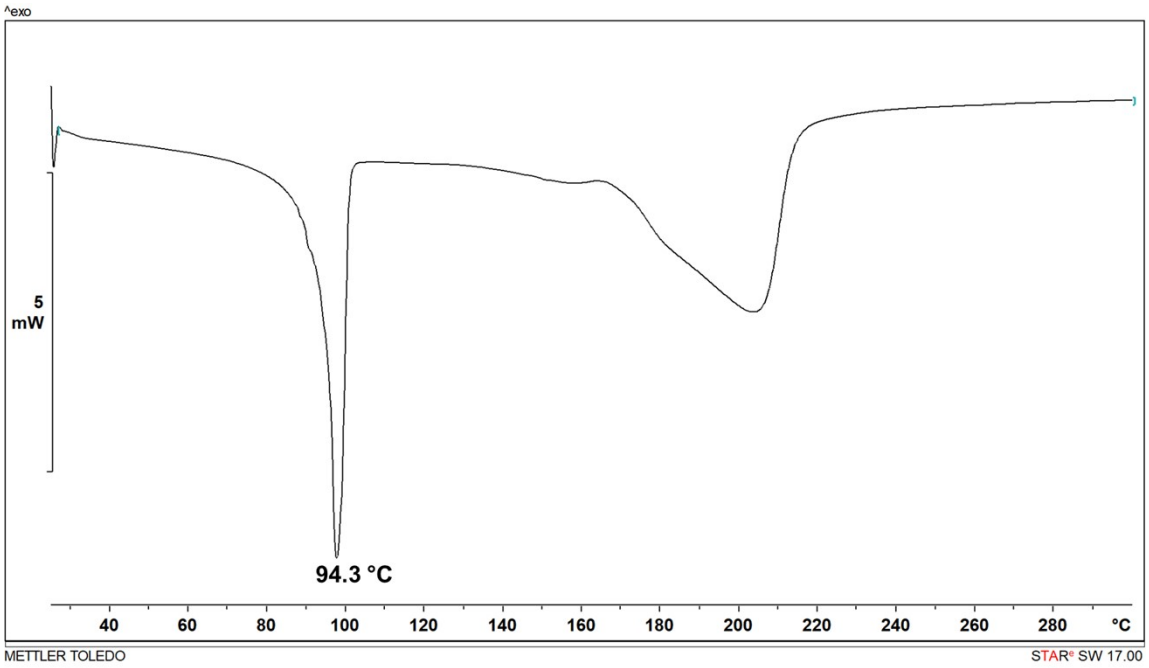

Figure S29. DSC curve of or crystal phases obtained by cocrystallized **pox** and **13tfib** in their respective stoichiometry

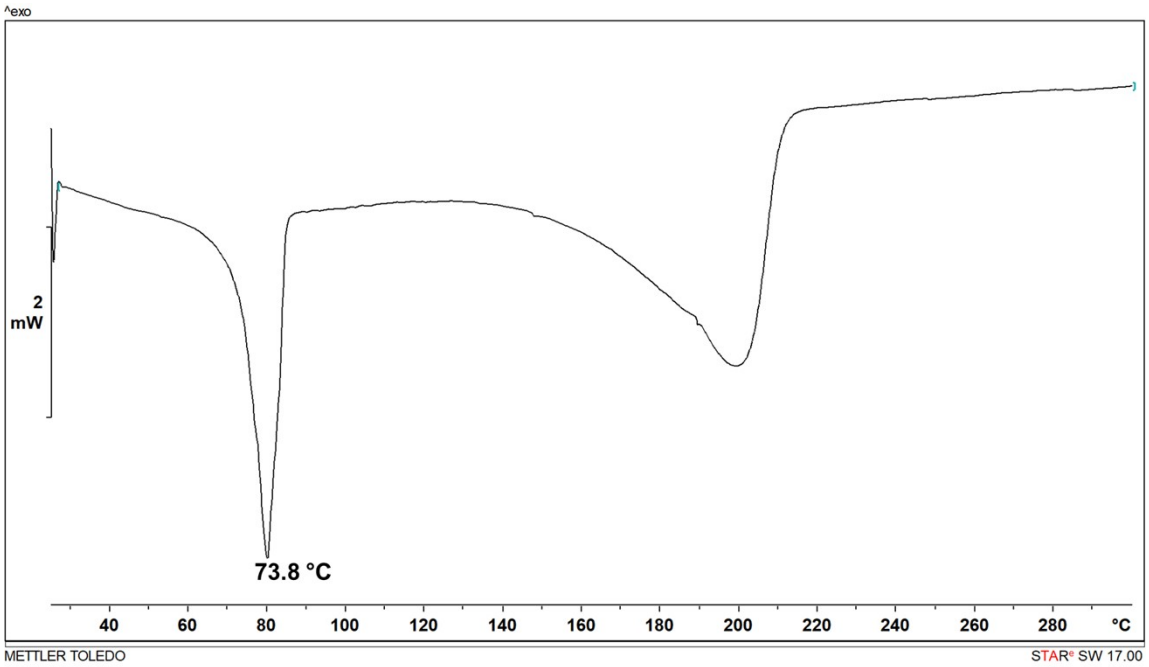

Figure S30. DSC curve of or crystal phases obtained by cocrystallized **tolox** and **14tfib** in their respective stoichiometry.

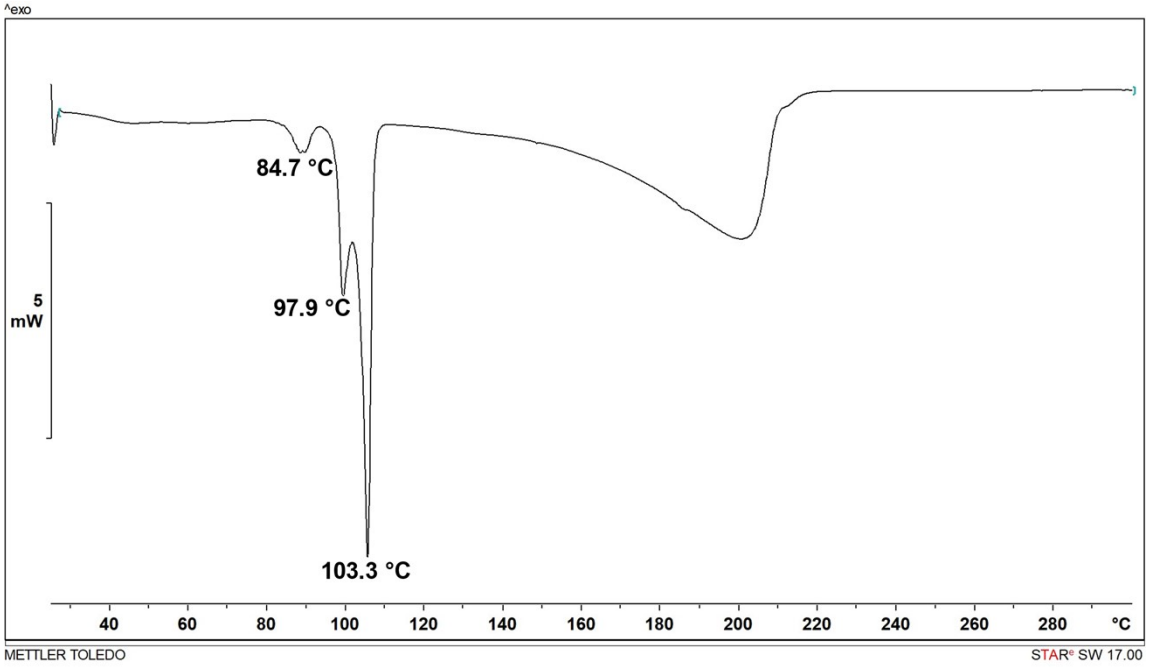

Figure S31. DSC curve of or crystal phases obtained by cocrystallized **nox** and **14tfib** in their respective stoichiometry.

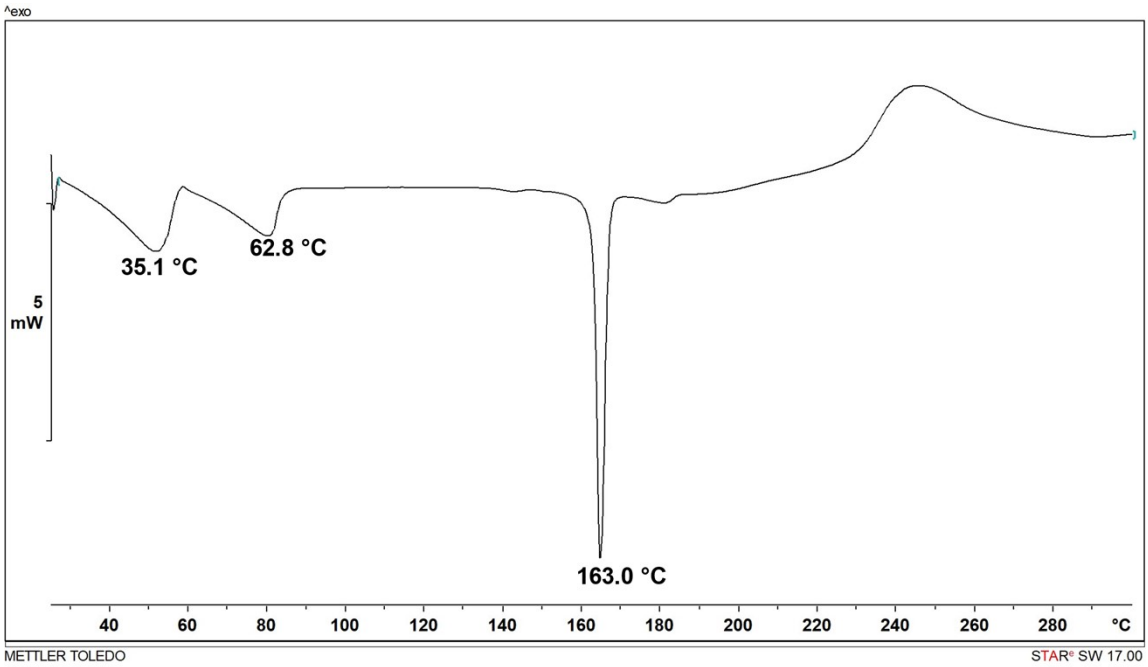

Figure S32. DSC curve of or crystal phases obtained by cocrystallized **nox** and **135tfib** in their respective stoichiometry.

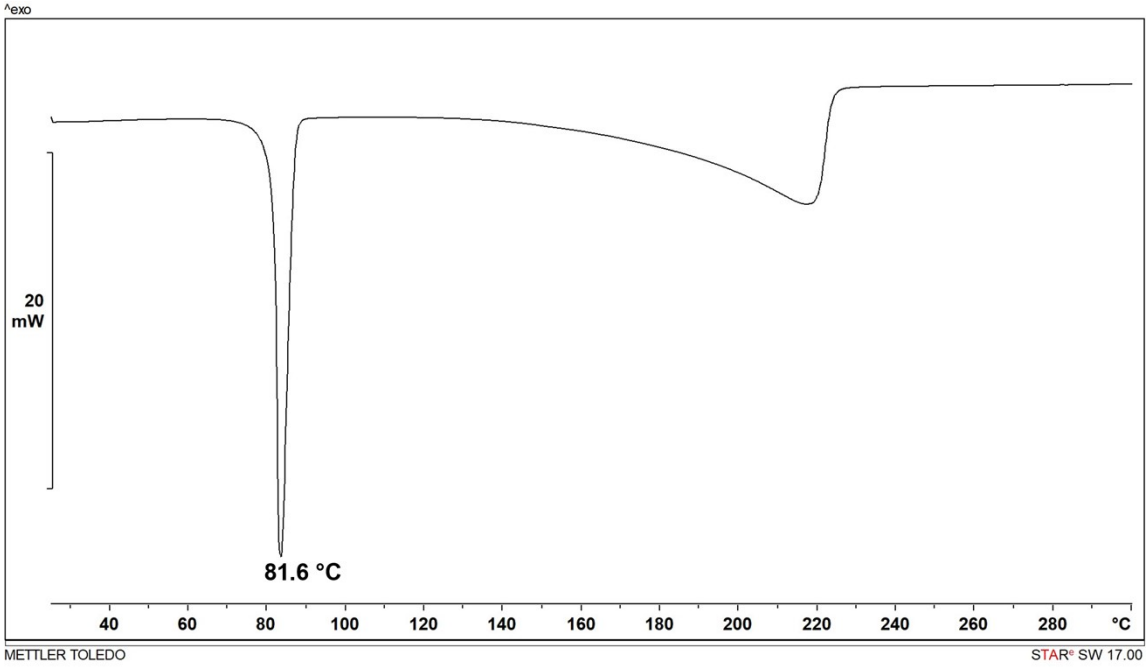

Figure S33. DSC curve of (**phox**)(**14tfib**).

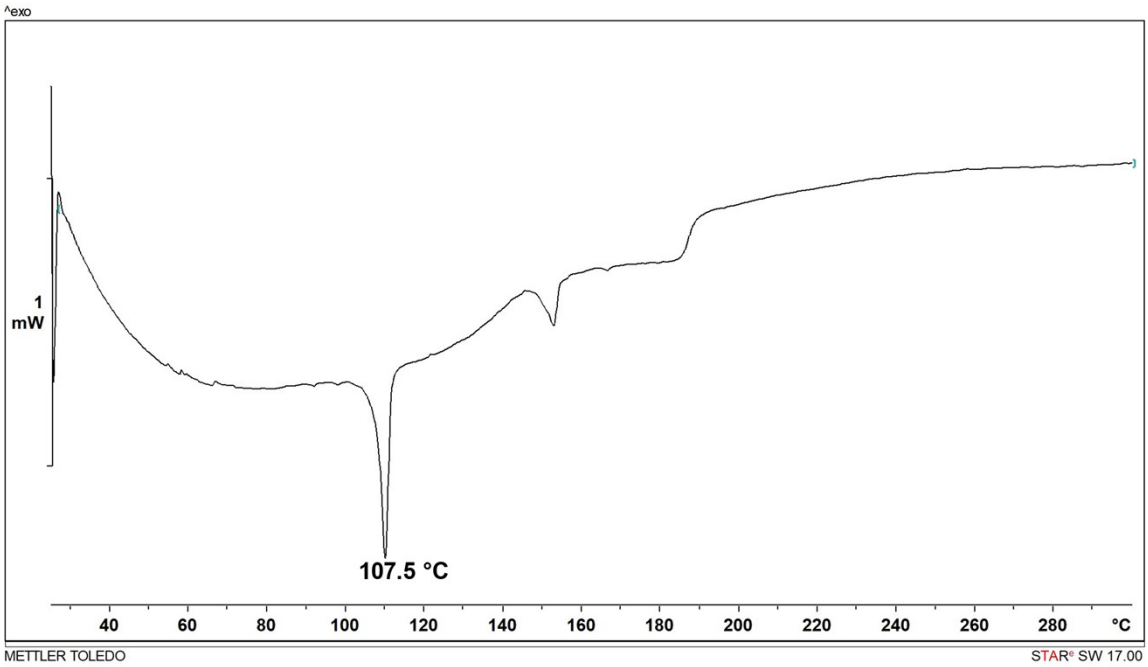

Figure S34. DSC curve of (**phox**)(**135tfib**).

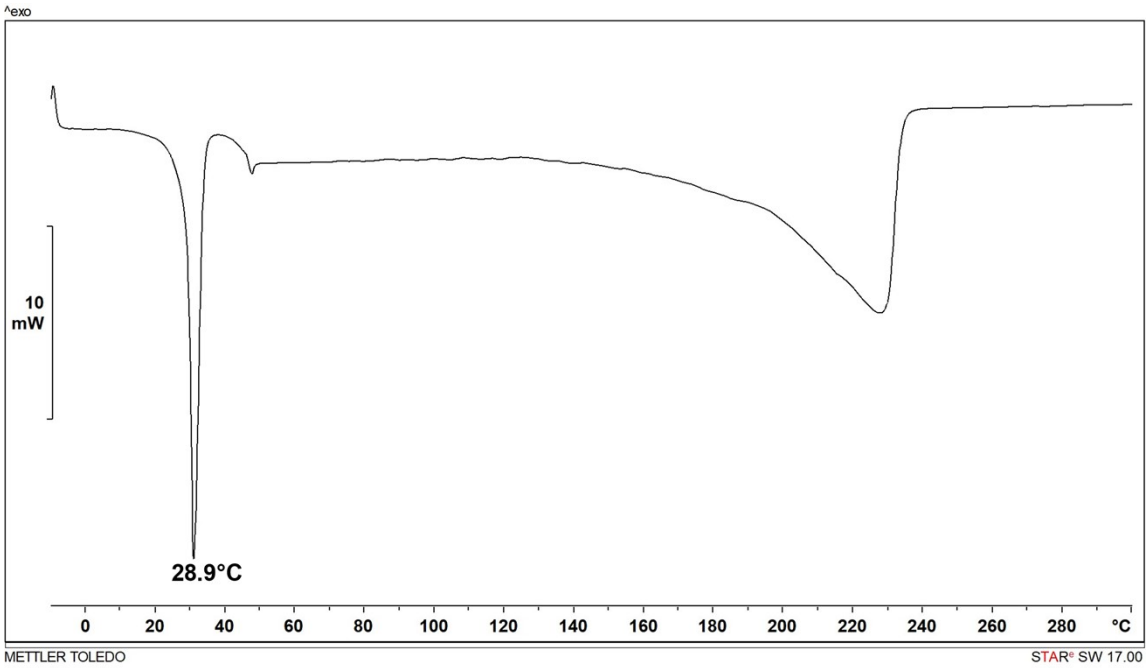

Figure S35. DSC curve of or crystal phases obtained by cocrystallized **phox** and **12tfib** in their respective stoichiometry.

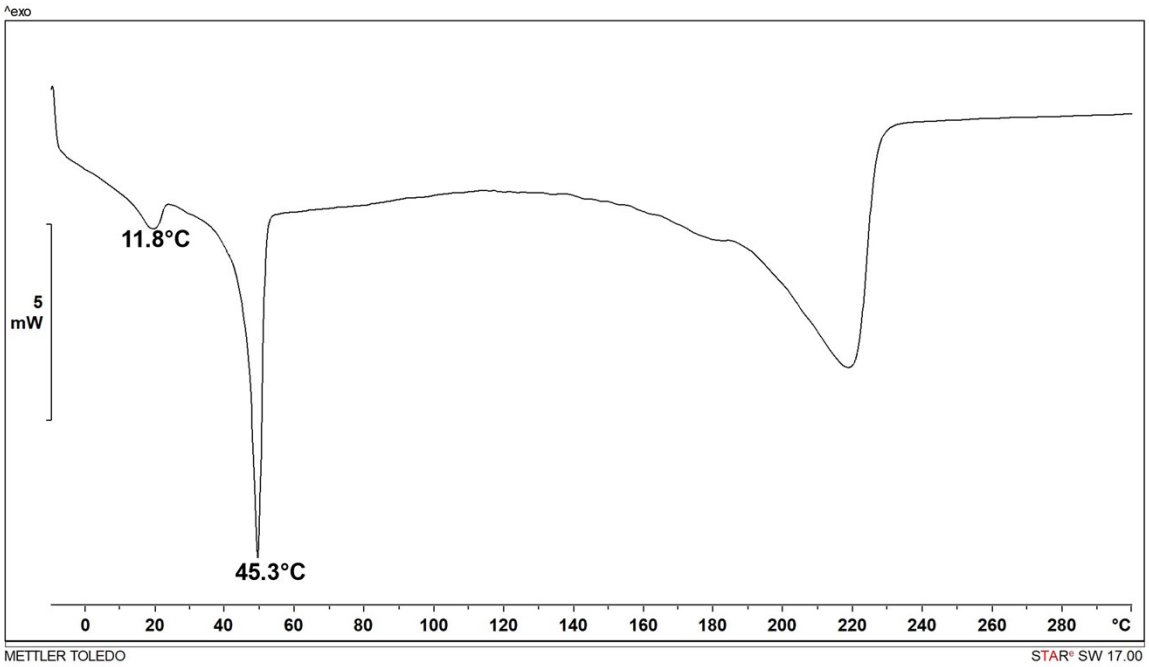

Figure S36. DSC curve of or crystal phases obtained by cocrystallized **phox** and **13tfib** in their respective stoichiometry

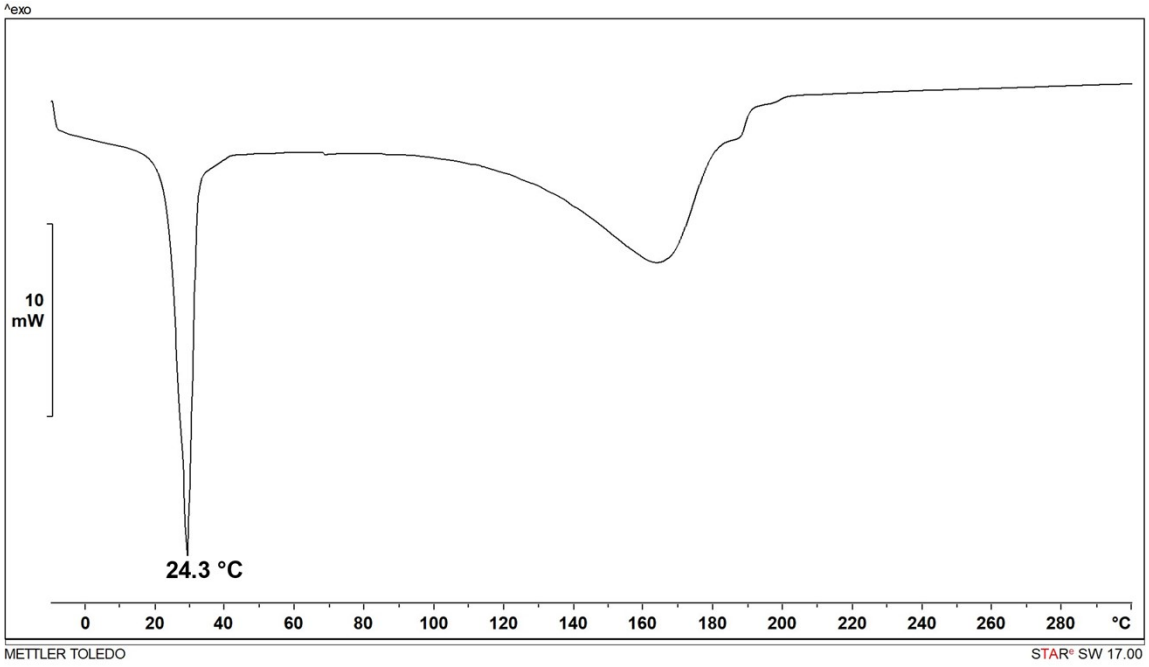

Figure S37. DSC curve of or crystal phases obtained by cocrystallized **box** and **14tfib** in their respective stoichiometry

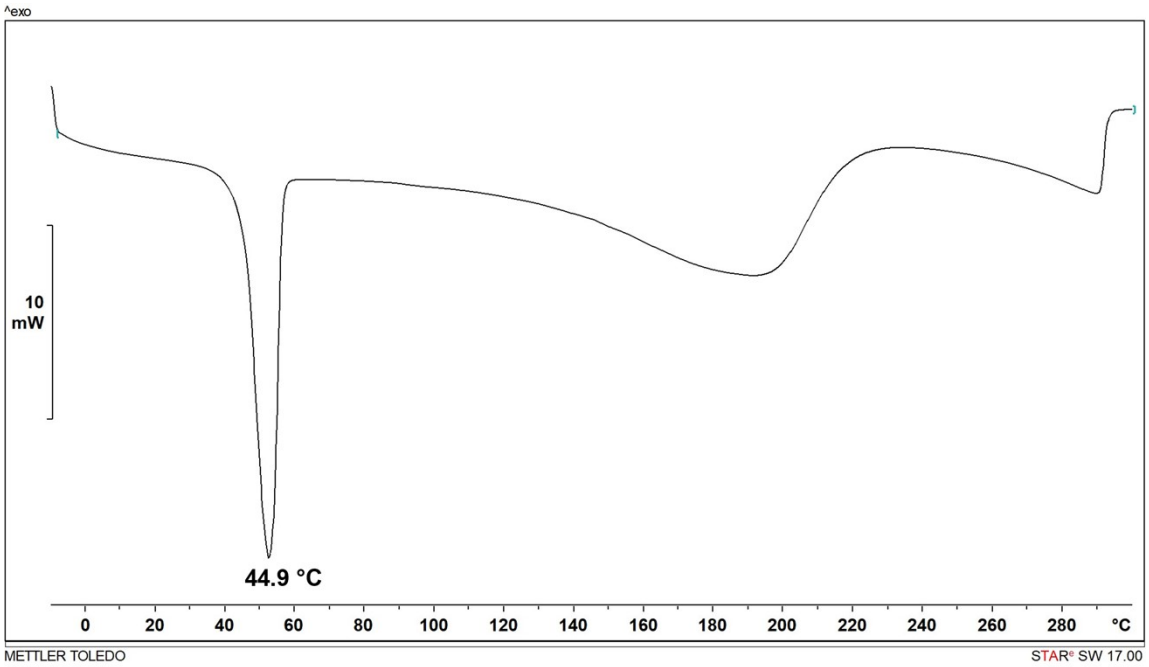

Figure S38. DSC curve of or crystal phases obtained by cocrystallized **box** and **135tfib** in their respective stoichiometry

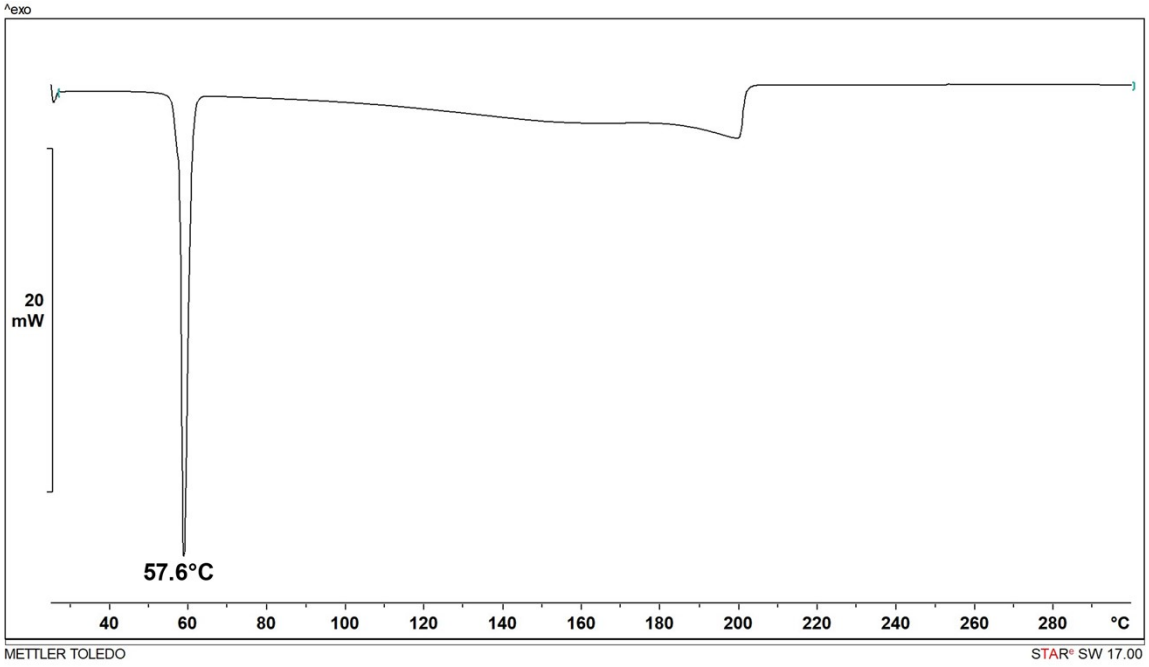

Figure S39. DSC curve of or crystal phases obtained by cocrystallized **box** and **12tfib** in their respective stoichiometry

PXRD patterns

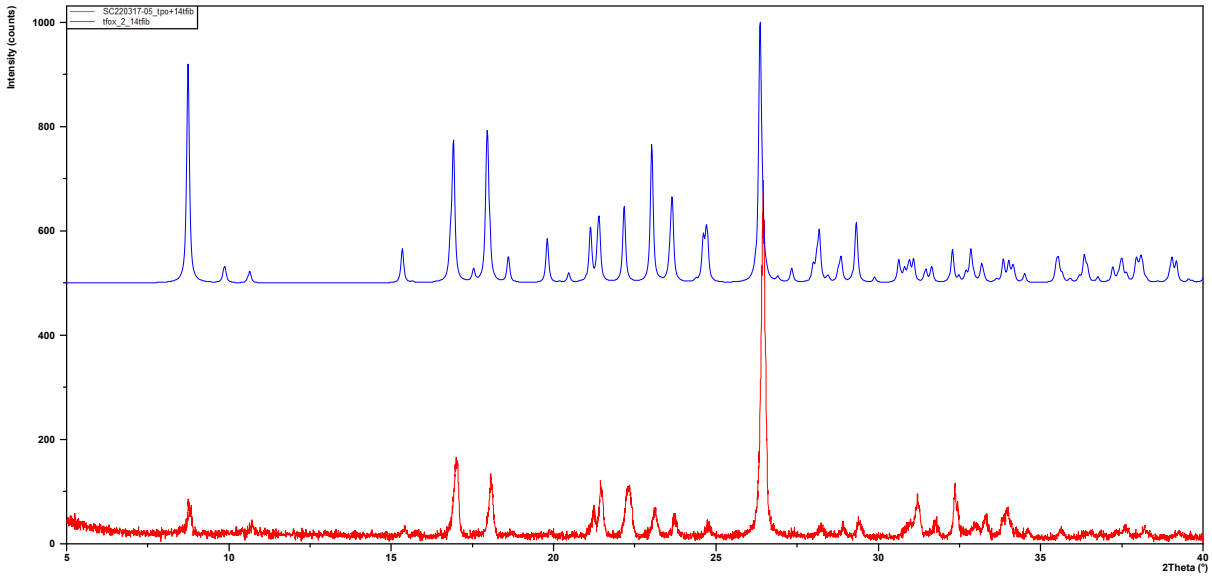

Figure S40. Calculated PXRD pattern from (**tfox**)$_2$(**14tfib**) single crystal data (blue) and diffractogram of the product obtained by crystallization (red)

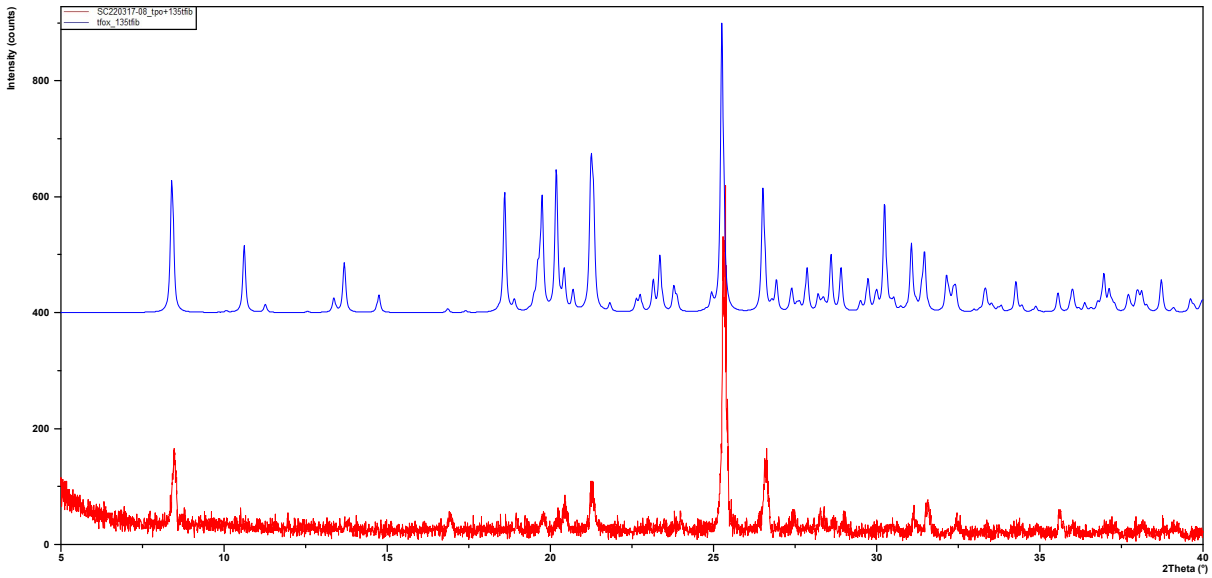

Figure S41. Calculated PXRD pattern from (**tfox**)(**135tfib**) single crystal data (blue) and diffractogram of the product obtained by crystallization (red)

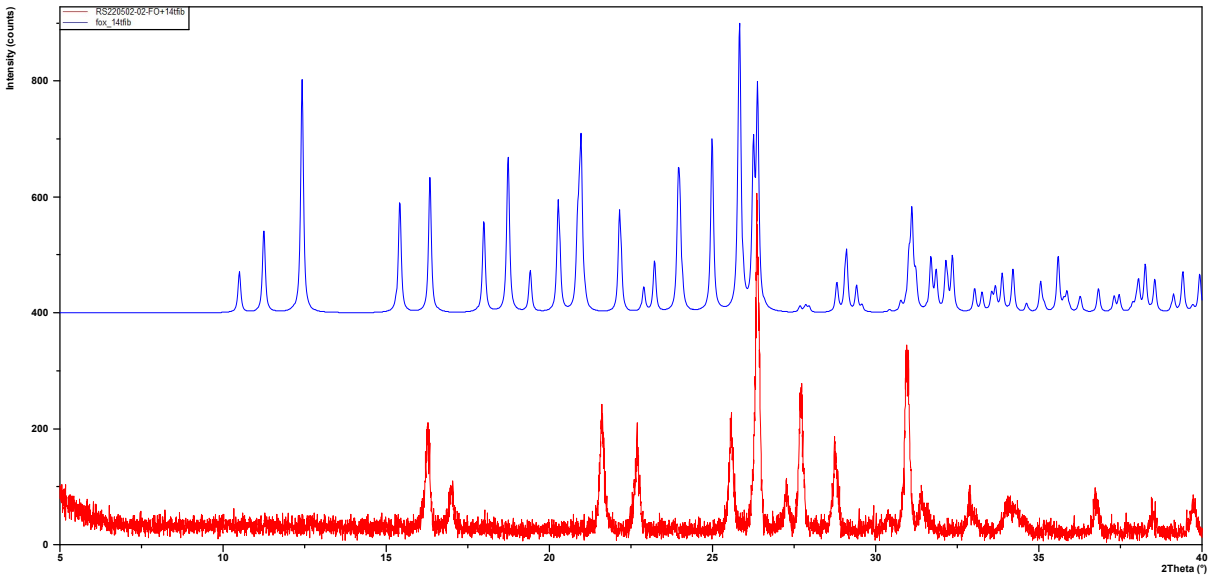

Figure S42. Calculated PXRD pattern from (**fox**)(**14tfib**) single crystal data (blue) and diffractogram of the product obtained by crystallization (red)

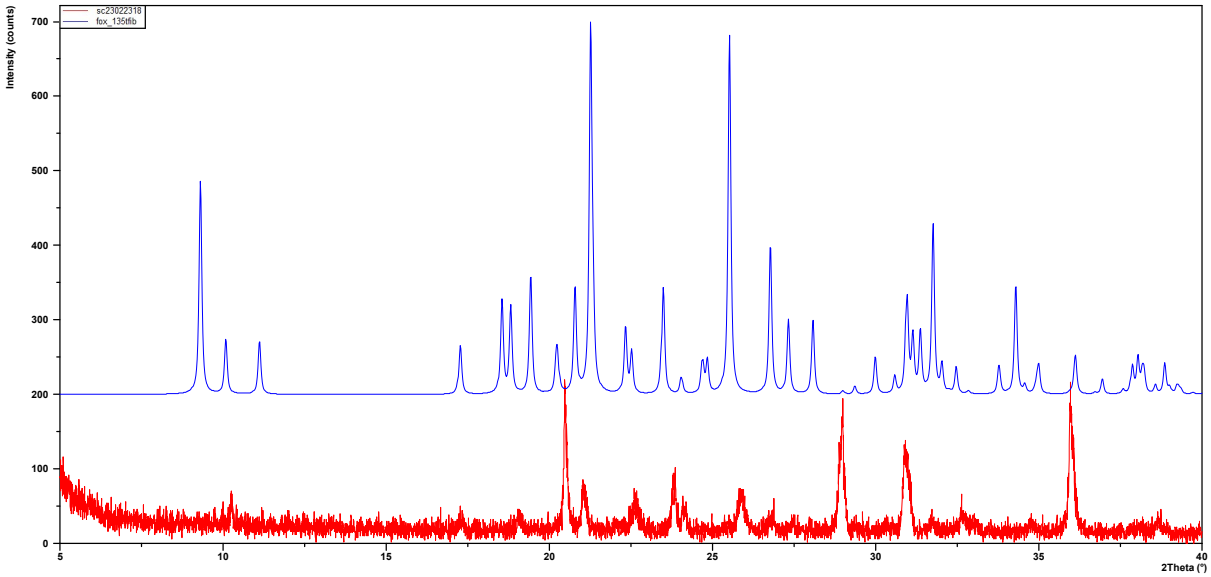

Figure S43. Calculated PXRD pattern from (**fox**)(**135tfib**) single crystal data (blue) and diffractogram of the product obtained by crystallization (red)

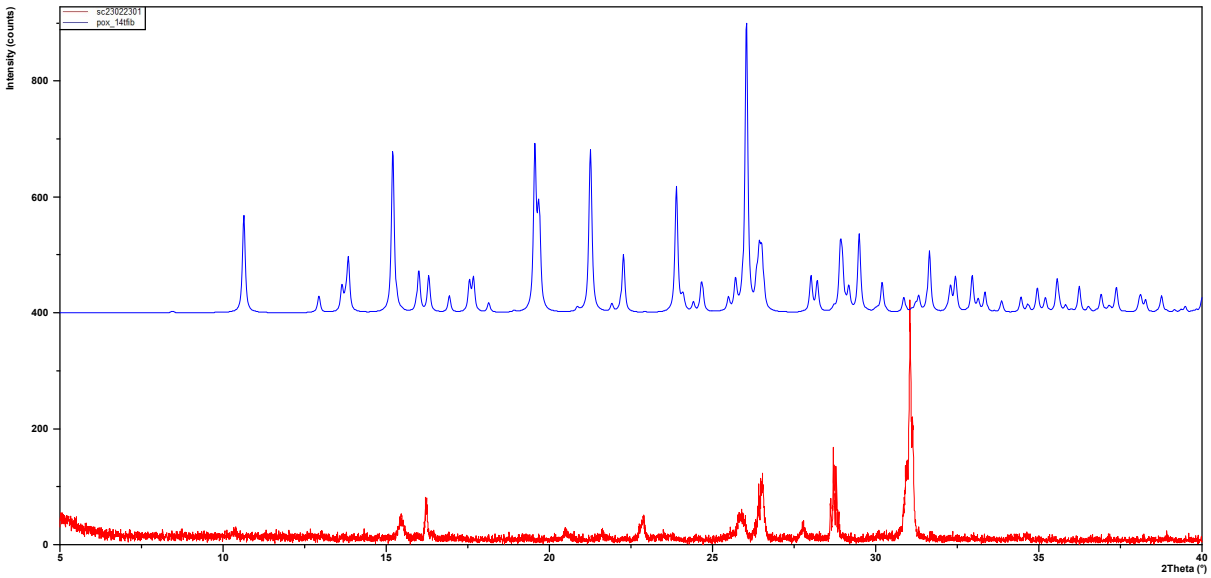

Figure S44. Calculated PXRD pattern from (**pox**)(**14tfib**) single crystal data (blue) and diffractogram of the product obtained by crystallization (red)

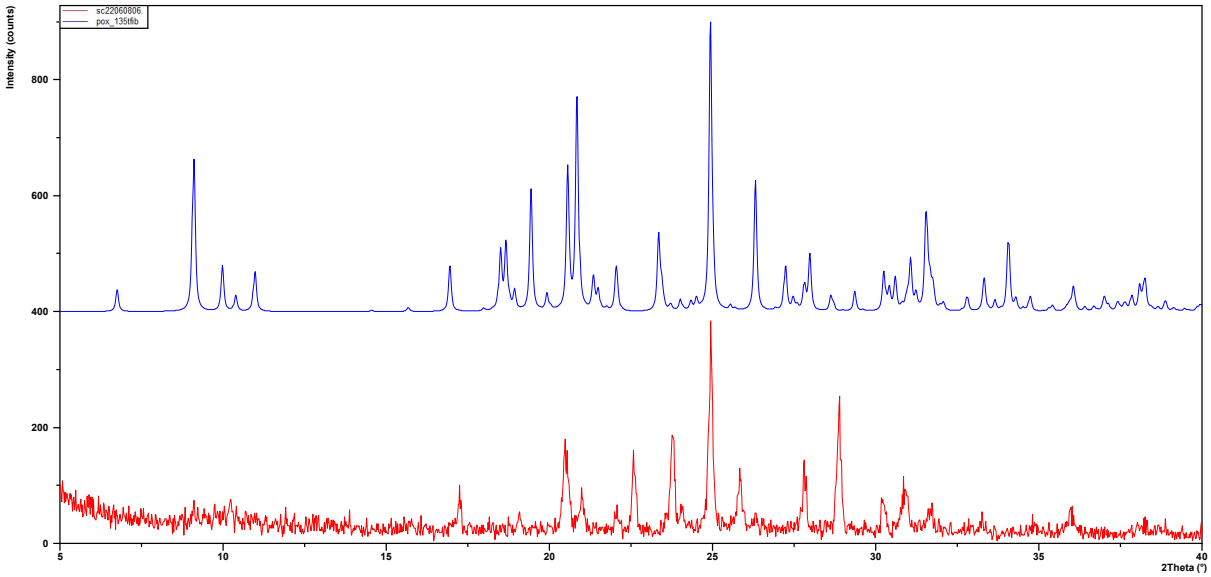

Figure S45. Calculated PXRD pattern from (**pox**)(**135tfib**) single crystal data (blue) and diffractogram of the product obtained by crystallization (red)

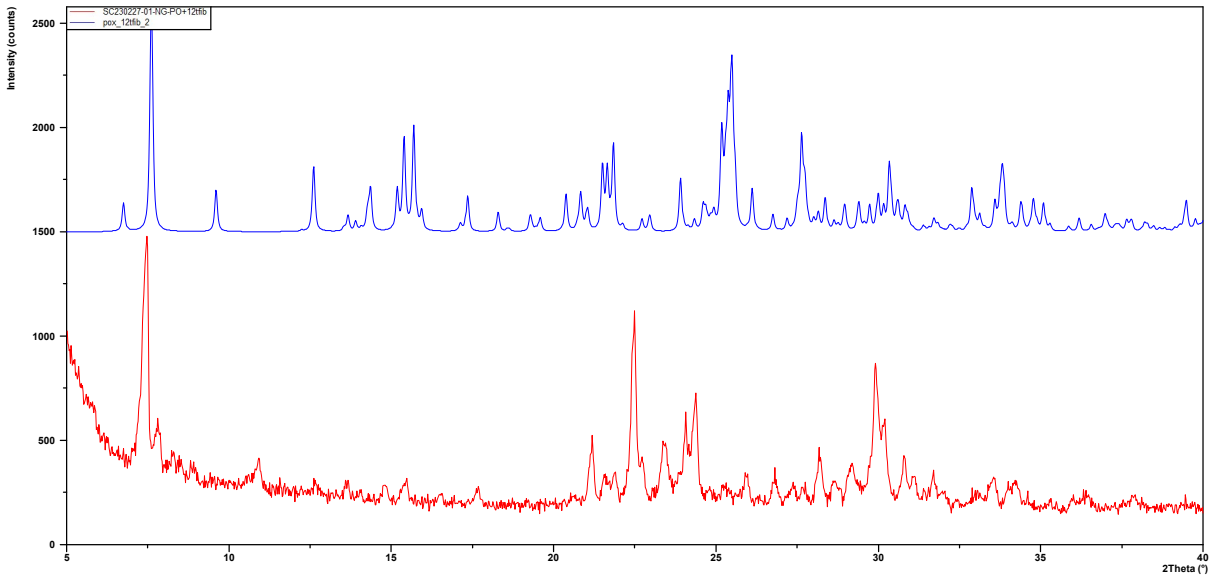

Figure S46. Calculated PXRD pattern from (**pox**)(**12tfib**)$_2$ single crystal data (blue) and diffractogram of the product obtained by crystallization (red)

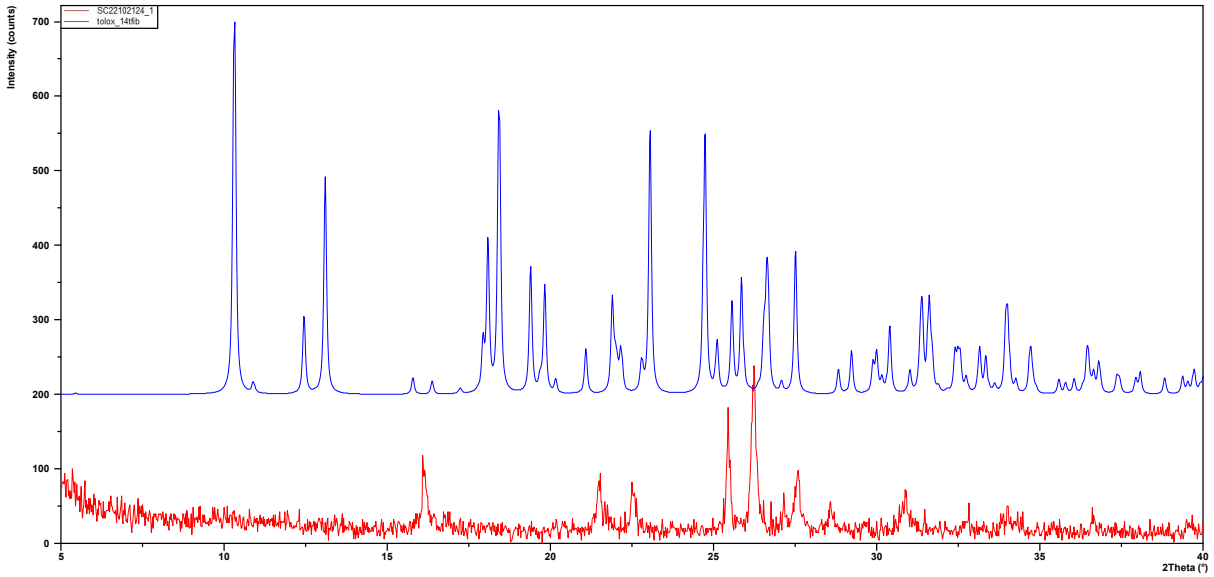

Figure S47. Calculated PXRD pattern from (**tolox**)(**14tfib**) single crystal data (blue) and diffractogram of the product obtained by crystallization (red)

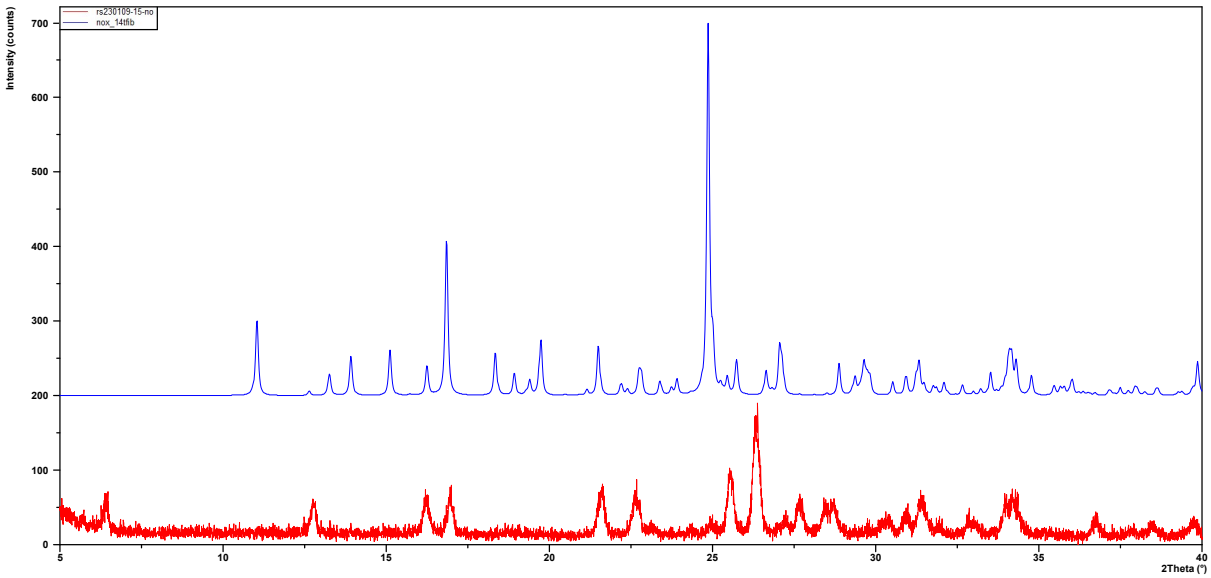

Figure S48. Calculated PXRD pattern from (**nox**)(**14tfib**) single crystal data (blue) and diffractogram of the product obtained by crystallization (red)

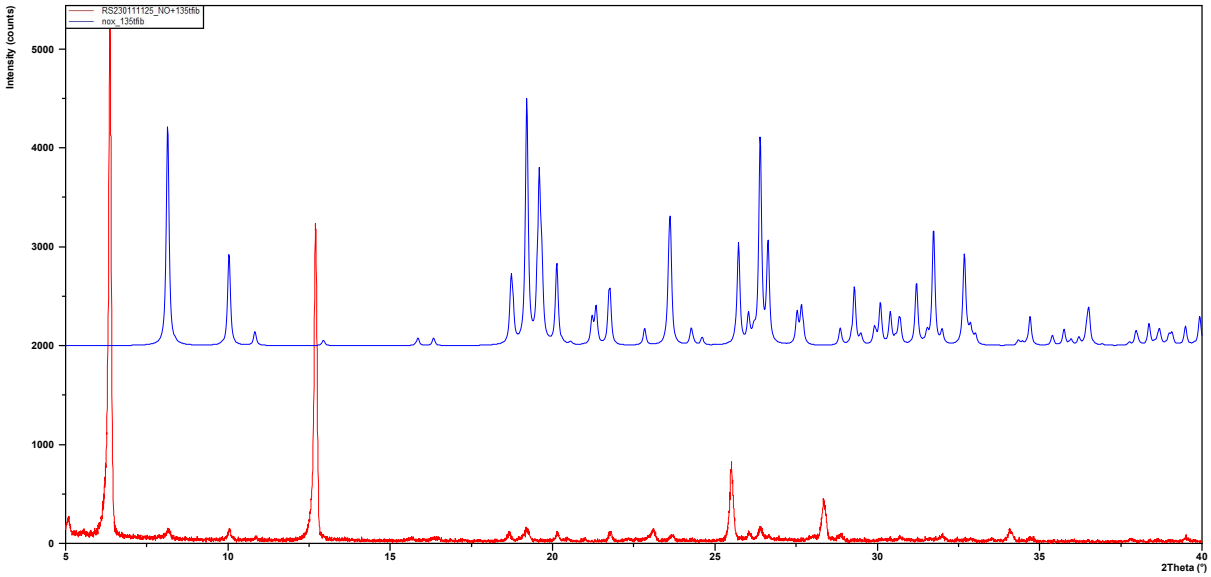

Figure S49. Calculated PXRD pattern from (**nox**)(**135tfib**) single crystal data (blue) and diffractogram of the product obtained by crystallization (red)

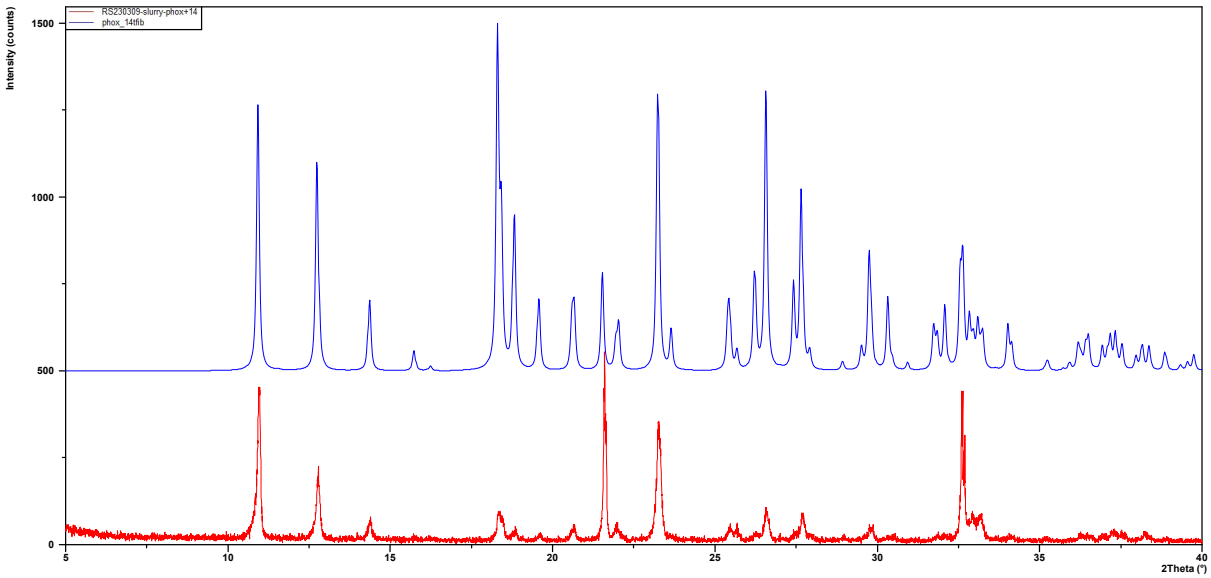

Figure S50. Calculated PXRD pattern from (**phox**)(**14tfib**) single crystal data (blue) and diffractogram of the product obtained by crystallization (red)

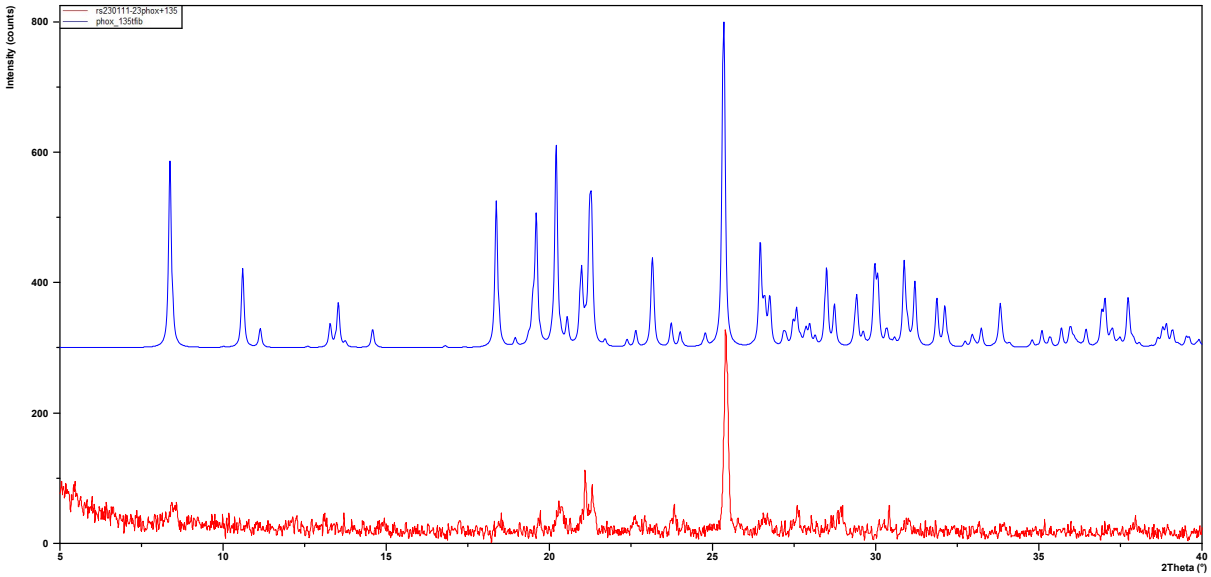

Figure S51. Calculated PXRD pattern from (**phox**)(**135tfib**) single crystal data (blue) and diffractogram of the product obtained by crystallization (red)

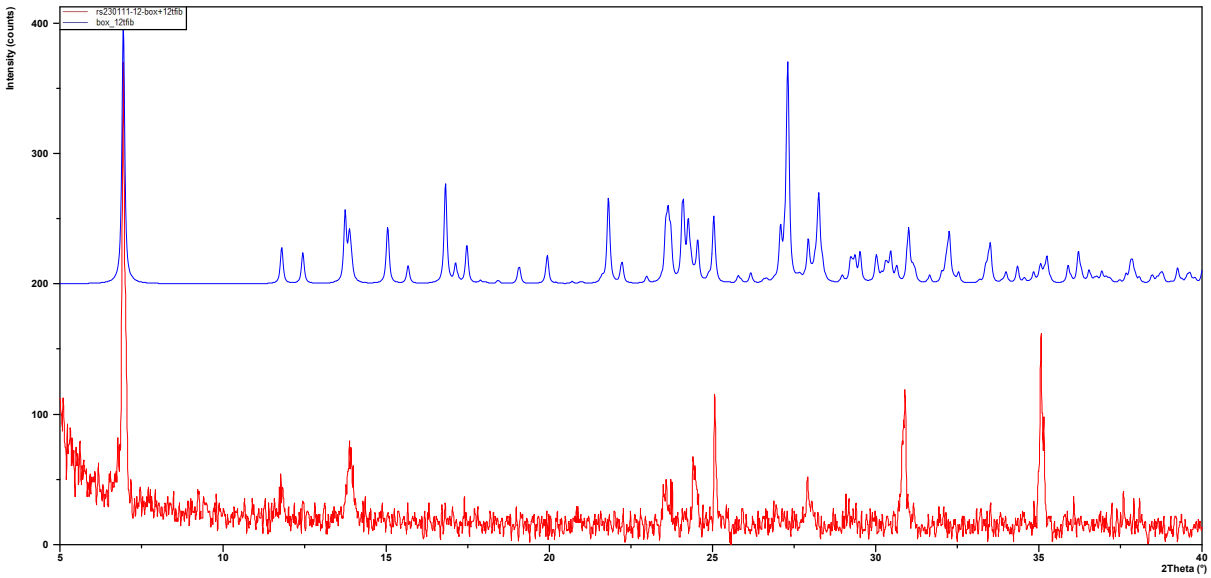

Figure S52. Calculated PXRD pattern from (**box**)(**12tfib**)$_2$ single crystal data (blue) and diffractogram of the product obtained by crystallization (red)

Table S3. Halogen bond energies between **14tfib** (model XB donor) and different acceptor sites on oxazoles used in study. Energies are BSSE corrected.

acceptor	E_{int} (I···$N_{oxazole}$)	E_{int} (I···$O_{oxazole}$)	E_{int}(I···periphery)
fox	–23.7	–10.08	–10.06
pox	–22.7	–10.46	–24.54
tfox	–23.79	–10.03	—
box	–23.53	–10.24	–14.96
nox	–20.99	–9.98	–15.41
tolox	–21.57	–10.11	—
phox	–23.67	–10.99	—

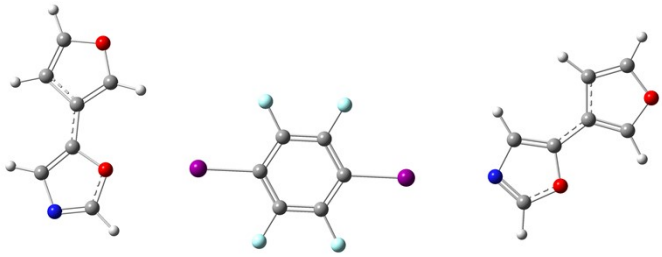

Figure S53. Optimized halogen-bonded trimer (**14tfib**)(**fox**)$_2$ including I···$N_{oxazole}$ and I···$O_{oxazole}$ halogen bonds.

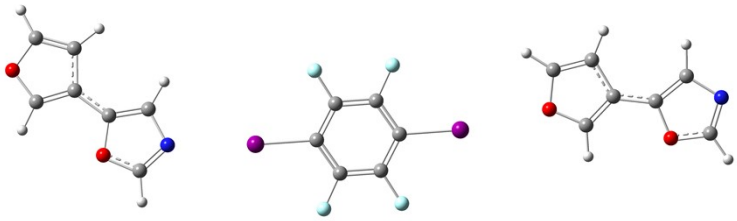

Figure S54. Optimized halogen-bonded trimer (**14tfib**)(**fox**)$_2$ including I···$N_{oxazole}$ and I···O_{furyl} halogen bonds.

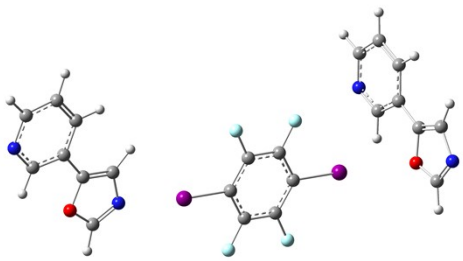

Figure S55. Optimized halogen-bonded trimer (**14tfib**)(p**ox**)$_2$ including I···$N_{oxazole}$ and I···$O_{oxazole}$ halogen bonds.

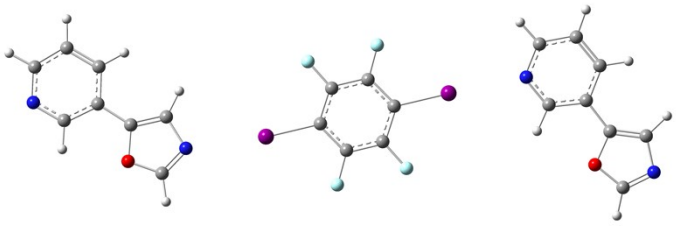

Figure S56. Optimized halogen-bonded trimer (**14tfib**)(**pox**)$_2$ including I···N$_{oxazole}$ and I···N$_{pyridyl}$ halogen bonds.

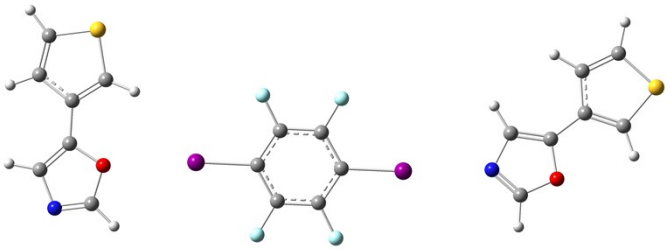

Figure S57. Optimized halogen-bonded trimer (**14tfib**)(**tfox**)$_2$ including I···N$_{oxazole}$ and I···O$_{oxazole}$ halogen bonds.

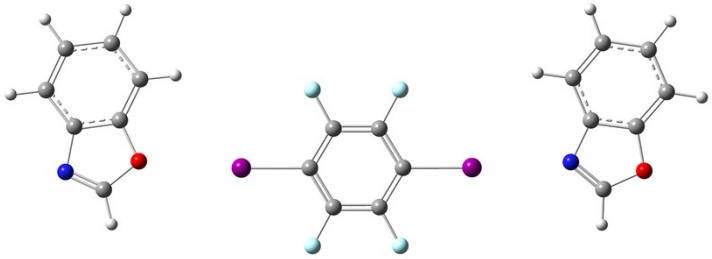

Figure S58. Optimized halogen-bonded trimer (**14tfib**)(**box**)$_2$ including I···N$_{oxazole}$ and I···O$_{oxazole}$ halogen bonds.

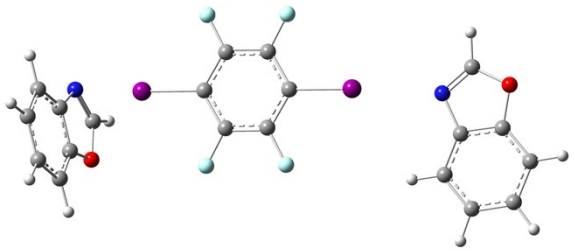

Figure S59. Optimized halogen-bonded trimer (**14tfib**)(**box**)$_2$ including I···N$_{oxazole}$ and I···π halogen bonds.

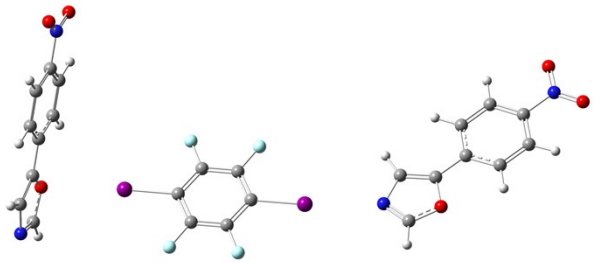

Figure S60. Optimized halogen-bonded trimer (**14tfib**)(**nox**)$_2$ including I···N$_{oxazole}$ and I···O$_{oxazole}$ halogen bonds.

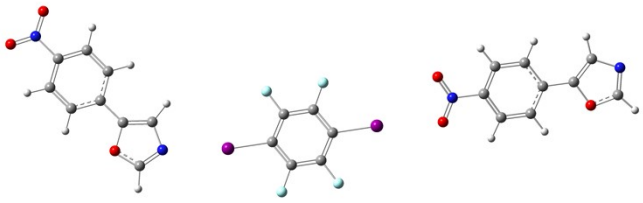

Figure S61. Optimized halogen-bonded trimer (**14tfib**)(**nox**)$_2$ including I···N$_{oxazole}$ and I···O$_{nitro}$ halogen bonds.

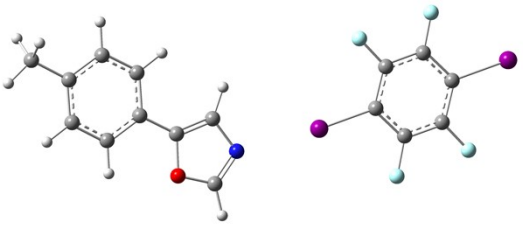

Figure S62. Optimized halogen-bonded trimer (**14tfib**)(**tox**) including I···N$_{oxazole}$ halogen bond.

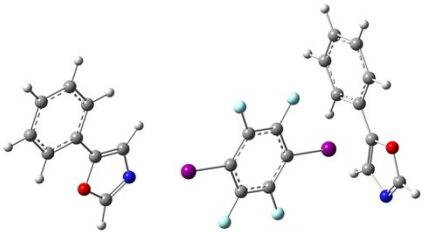

Figure S63. Optimized halogen-bonded trimer (**14tfib**)(**phox**)$_2$ including I···N$_{oxazole}$ and I···O$_{oxazole}$ halogen bonds.